UNIVERSITY OF THESSALY

DEPARTMENT OF MECHANICAL ENGINEERING

EFFECT OF BAINITIC ISOTHERMAL TRANSFORMATION PARAMETERS ON THE FRACTURE BEHAVIOR OF ALUMINUM CONTAINING TRIP700 STEEL

STEFANOS GONIDAKIS

M. Sc. Thesis

2017

Approved by the members of the Examination Committee

First Examiner (Supervisor)	Dr. Alexis Kermanidis Assistant Professor, Department of Mechanical Engineering, University of Thessaly
Second Examiner	Dr. Nικolaos Aravas Professor, Department of Mechanical Engineering, University of Thessaly
Third Examiner	Dr. Michalis Agoras Assistant Professor, Department of Mechanical engineering, University of Thessaly

Abstract

Transformation induced plasticity (TRIP) steels have excellent strength and ductility accompanied by a gradual work hardening behavior, which can be attributed to the TRIP phenomenon. The metastable retained austenite transforms into martensite as a result of applied stress or strain and the obtained transformation absorbs energy and toughens the material, thus improving the work hardening rate and delaying the necking effect. The TRIP effect is the result of the RA microstructure obtained during bainitic transformation that is characterized by the size of RA particles, initial RA content and its stability against transformation.

In the present work the influence of isothermal bainitic transformation parameters on the TRIP steel microstructure have been examined and subsequently on the fracture behavior of an aluminum containing TRIP steel. In order to obtain the desired differences in microstructure, a two-step heat treatment procedure has been implemented using different temperatures and times in the bainitic transformation region to produce variation in the TRIP steel microstructure. The microstructure morphology of the TRIP steel materials was characterized using standard metallographic techniques. Firstly, the effect of heat treatment process on the tensile behavior of the material was evaluated and subsequently the fracture behavior was investigated under static and cyclic loading conditions. Typical load vs crack opening displacement diagrams were determined to evaluate the role of microstructure on the tearing resistance and fatigue crack growth behavior of the TRIP steel. The results indicate that a microstructure with relatively stable RA acts in favor of the fracture resistance against static loading, while fatigue crack growth resistance is supported by the transformation effect.

Acknowledgements

First and foremost, I would like to express my sincere gratitude to my supervising Assistant Professor Alexis Kermanidis for the continuous support of my Master study and related research, for his patience, motivation and immense knowledge. There are no words which can describe my appreciation to him. His guidance helped me in all the time of the research and writing of this thesis. He showed a strong belief in my potentials and gave me the opportunity to carry out experiments in Trip steel material. He has devoted much time in order to help me complete this thesis and for that reason I am indebted to him.

I would like to thank prof. G. N. Haidemenopoulos for the permission to use the Materials Laboratory and his guidance and support with the heat treatment procedure

I would also like to thank the members of the examination committee Prof. N. Aravas and Assistant Prof. Michalis Agoras.

Special regards to Voestalpine Stahl company, which is located in Linz. Austria and Dr. Daniel Krizan for the SM measurements

Ph.D. student Peter Christodoulou for his assistance in order to optimize my skills in tensile and fracture testing with the Instron Force Testing machine and his support to my research.

I would like to express my gratitude to Dr. Eleni Kamoutsi for the assistance and support with metallography procedure and hardness measurements.

The Leventeris Company for the protection clothing which lend me in order to accomplish the heat treatments safely.

The Lazarou bros company for the specimen preparation.

My supervisor Dimitris Mouratidis of Quality Control from Lafarge Holcim company for his advice, support and flexibility he provided to me with my dismissal from work in order to complete this task while working.

Lastly, I would like to thank my fiancé Alexia for her support all this time, my parents Jonh and Chysoula, my sister Anna and my best friend Sotiris

Table of contents

1 Introduction

1.1 Objective

TRIP steels offer an outstanding combination of strength and ductility as a result of their microstructure making them suitable in the automotive industry for the production of structural and reinforcement parts of complex shapes.

At present they are used for automotive structural and safety parts such as cross members, longitudinal beams (members that are slender and support loads applied perpendicular to their longitudinal axis), B-pillar reinforcements, bumper reinforcements, figure 1.1.

Figure 1.1: The applications of TRIP steels in automotive industry, in the [left] picture front bumper, [center] picture B pillar, [right] cross members.

The microstructure is composed of austenite islands and carbide-free bainite dispersed in a soft ferritic matrix. Austenite is transformed into martensite during plastic deformation as a result of the TRIP effect (Transformation Induced Plasticity), which is responsible for their excellent mechanical behavior.

Transformation of retained austenite (RA) is controlled by several microstructural influences that include initial RA volume fraction, size of RA and its stability and the way the retained austenite is dispersed inside the austenitic grains. The chemical composition is also important and is linked to the chemical stability of retained austenite.

The TRIP steel microstructure is a product of a specific heat treatment procedure that includes annealing in the intercritical region of the material among the

Ac1 and Ac3 temperature transformations and holding in the isothermal bainitic region. Parameters such as the temperature and time in the bainitic transformation region determine the final content of RA as well as its stability against transformation. In order to improve the understanding of the microstructural influence of the TRIP effect on mechanical behavior, heat treatment parameters in the bainitic transformation region have been investigated by designing different heat treatment procedures of the TRIP steel and then the material performance was evaluated. More specifically, microstructural investigation of the materials produced with the different heat treatment parameters has been conducted and the mechanical behavior including tensile and as well as static and cyclic fracture tests has been examined.

1.2 Outline

The thesis includes in total 5 chapters. In chapter 1 an introduction to the problem is attempted including an outline of the present work.

In chapter 2 is included a brief introduction about the TRIP steels and their validity in the automobile industry. General information is pointed about the microstructural components, the importance of elements concentrations in the chemical composition, the optimal heat treatment procedures of TRIP steels, aspects of the martensitic transformation as well as several parameters that influence the austenite stability. Also articles from other researchers are discussed about fracture behavior and crack propagation under constant loading in TRIP steels.

In chapter 3 the experimental program is analyzed which consists of two parts. The first part is dedicated to the design and implementation of heat treatment procedure to produce TRIP steel microstructures with different RA characteristics and their microstructural evaluation. The second part deals with the investigation of mechanical behavior of the produced TRIP steels and includes examination of the static (tensile) and fracture behavior (fracture toughness and fatigue crack growth).

In chapter 4 the experimental results produced using the techniques described in chapter 3 are presented and discussed.

In chapter 5 the basic conclusions of the investigation are summarized and suggestions for further work are given.

2 Literature review

2.1 Introduction

Climate changes due to modern society pollution have driven automotive industries to produce more fuel efficient vehicles. One method of achieving this objective is by reducing the weight of the vehicle body, thereby reducing its fuel consumption and greenhouse gas emissions. Road vehicles, especially passenger cars, can potentially bring about the highest energy savings because they are the highest contributor to transport energy consumption due to the sheer number of these vehicles on the road. In order to fulfil these goals, the development of new materials with improved formability and increased strength is required. The TRIP steels are a new category of Advanced High Strength Steels (AHSS) [1], with the above characteristics, their excellent properties being a result of the Transformation Induced Plasticity (TRIP) phenomenon.

Advanced high-strength steels (AHSS) have both high strength and ductility in comparison to conventional steels as shown in figure 2.1

An important factor of such steel technology is the ability of the material to form under pressure and acquire shapes capable for being implemented on a car body. Thus by producing steels with higher strength and ductility the formability may be improved and thinner sheets can be manufactured for structural components by maintaining structural integrity. Consequently, the weight of the car body can be reduced. In this direction the TRIP steels as it is depicted in Figure 2.1 are a very promising alternative.

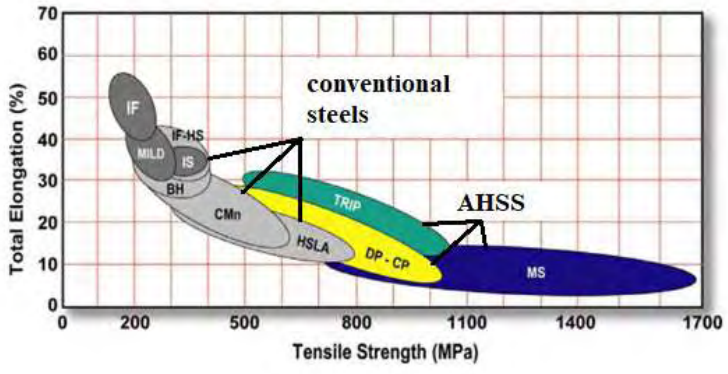

Figure 2.1: Mechanical properties of AHSS [1]

2.2 Mechanical properties of TRIP steels

TRIP steels provide a good combination of strength, ductility and work hardening properties than other first generation AHSS. Their application in the automotive industry is in reinforcement parts of the vehicle steel chassis as shown in figure 2.2.

Figure 2.2: Car components manufactured from Trip steels [2]

TRIP steels exhibit high values of uniform elongation with a progressive strain hardening which are accompanied by a high ultimate tensile strength (UTS) (figure 2.3), in comparison with conventional and dual phase steels, making them an excellent candidate for automotive applications. Structural components can be made thinner because of the combined strength and steel ductility to withstand high deformation processes. In addition to advantages of using TRIP steel for reducing vehicle weight, their energy absorption behavior is ideal for improving the passive and active safety of vehicles. The excellent energy absorption characteristics and high work hardening response improves the crashworthiness of a vehicle [3].

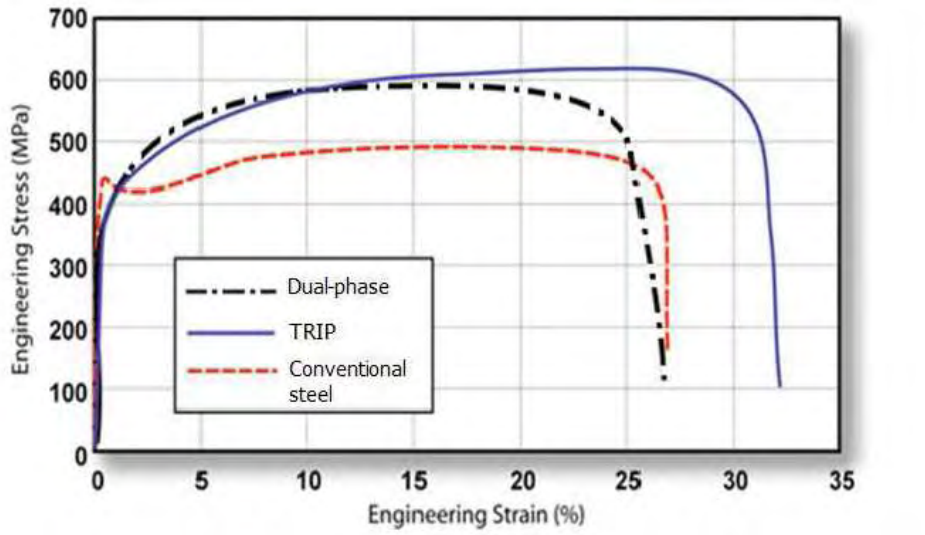

Figure 2.3: Comparison of stress-strain curves [1]

2.3 Microstructure

The TRIP effect depends on the chemical composition and the two-stage heat treatment procedure which result to a microstructure with an initial RA content and stability which is influenced by the process parameters.

The microstructure of TRIP steels consists of body-centered cubic (BCC) ferrite which is the softest phase among the other constituents, the bainite which is formed by fine ferrite platelets and cementite (Fe_3C) precipitating between and inside the ferrite plates and the austenite in face-centered cubic lattice which is usually stable in high temperatures.

The bainite forms inside the soft ferritic matrix accompanied by the formation of carbides around the bainitic ferrite. In TRIP steels as bainite forms, carbon is partitioned in the surrounding austenite. The carbides are inhibited by the additions of other alloy elements preventing their formation from occurring and the carbon is partitioned directly into the austenite. The austenite is normally stable at high temperatures as mentioned before, but the enrichment of carbon and the stresses from the nearby grains can stabilize the austenite at room temperature. The austenite fraction in TRIP steels is called retained. The unique properties of TRIP steels are mainly due to the presence of the metastable austenite phase stabilized in room

temperature. An electron microscopy picture of a typical TRIP microstructure is shown in figure 2.4 (the material was delivered by Voestalpine).

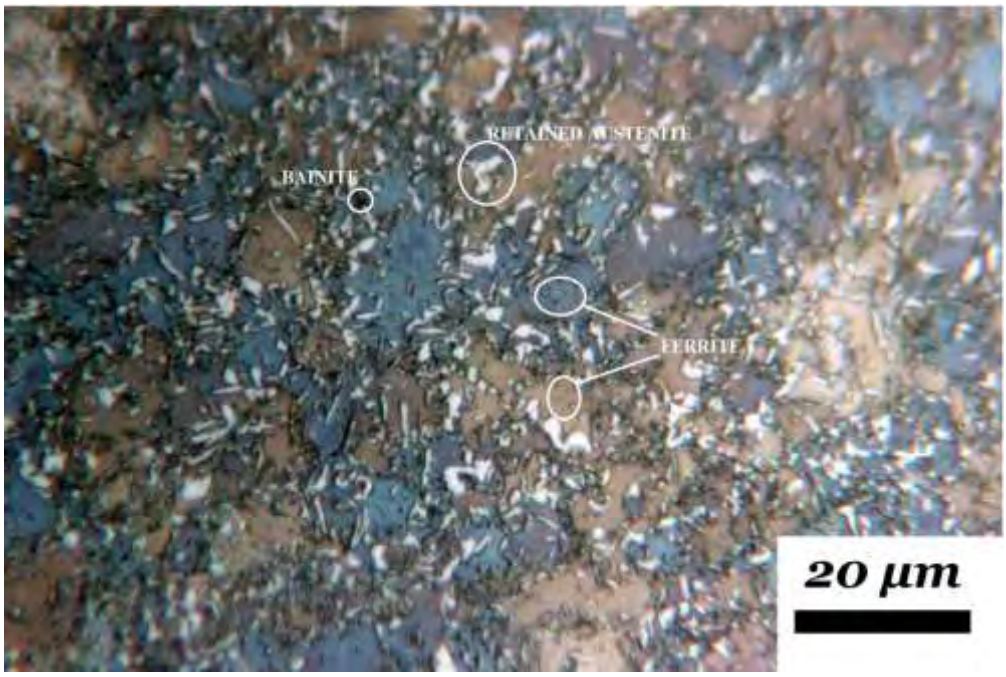

Figure 2.4: Typical microstructure of a TRIP700 steel used in the present study

2.4 Heat treatment

In order to obtain the typical multi-phase TRIP steel microstructure, a two-step heat treatment is required. The final properties of the material depend on the volume fraction of the retained austenite, its morphology and the carbon content that provides the TRIP effect during deformation. The heat treatment is designed specifically to transform the carbide precipitation into carbon enriched austenite phase so that is stabilized to room temperature.

The first stage of the heat treatment path consists of intercritical annealing, in the temperatures between Ac1, first transformation temperature (from BCC solid solution to BCC + FCC solid solution, austenite and ferrite fraction,) and Ac3 (from BCC + FCC solid solution, to austenite γ FCC), followed by the second stage of the heat treatment an isothermal bainitic hold and cooling. The annealing temperature for the first step of the heat treatment is chosen inside the intercritical region of the Fe-C phase diagram (shown as the region labelled γ + α in Figure 2.5). This is the

temperature range in which both ferrite (α) and austenite (γ) are present in the microstructure. The intercritical region is between the transformation temperatures Ac1 and Ac3. Ac1 is the lower transformation temperature, where austenite begins to form during heating of the steel. Ac3 is the upper boundary of the intercritical region and is the temperature at which the transformation of ferrite to austenite is completed upon heating. Those two temperatures depend on the chemical composition of the TRIP steels. The initial microstructure of the material also influences the kinetics of cementite during dissolution and hence the saturation of austenite phase with carbon. The resulted refined microstructure of the carbides after rapid cooling accelerates the kinetics of intercritical annealing process and saturated the austenite with carbon during subsequent reheating [4].

The standard heat treatment procedure is shown schematically in Figure 2.6 along with diagrams depicting the microstructure development over the course of the heat treatment and a transformation analysis occurring in each segment of the diagram. This heat treatment path and the chemical composition are designed to promote the formation of carbon-saturated austenite which can be retained in the microstructure when the steel is subjected to room temperature. In the annealing procedure between the intercritical region the austenite fraction is saturated with the carbon content. According to research soaking should not be accompanied with prolonged time. Increasing intercritical soaking periods, increase the austenite volume fraction coarsens the grain, which reduces the austenitic stability. The stability of the RA can be preserved by the small grain sizes and high carbon content [5].

The second step of TRIP steels heat treatment is to hold the material within the range of isothermal bainitic transformation. The kinetics in the bainitic region are affected by the chemical composition. Soaking at high temperatures in the bainitic region TRIP steels tent the upper bainite formation is appeared. At the beginning of holding in the bainite region, there is a large amount of remaining austenite. However, the carbon level in this austenite is still too low and therefore the martensite start (MS) temperature of that austenite is relatively high. The bainitic transformation decreases the MS below the room temperature by enriching the austenite with carbon. The enrichment of the austenite is due to the low alloy concentration in the TRIP steel chemical composition which prevents the carbide formation and increase carbon partitioning. This mechanism leads to a microstructure containing ferrite, bainite and

retained austenite. The longer the soaking time in the BIT, the greater the extent of completion of bainitic transformation and the lower the amount of remaining austenite. As the bainitic transformation progresses, the stability of high-carbon retained austenite increases until it reaches maximum, while the volume fraction decreases [6].

An increased intercritical temperature causes grain coarsening and increasing the volume fraction of the retained austenite. In BIT increased holding time lead to a decrease of strength and increase of toughness. [7].

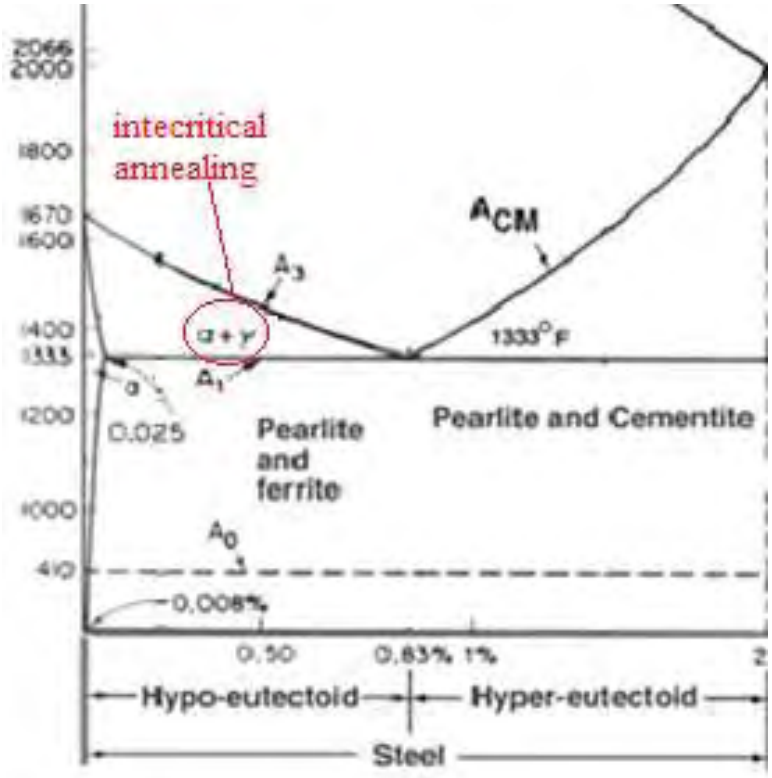

Figure 2.5: Carbon-Steel phase diagram [8]

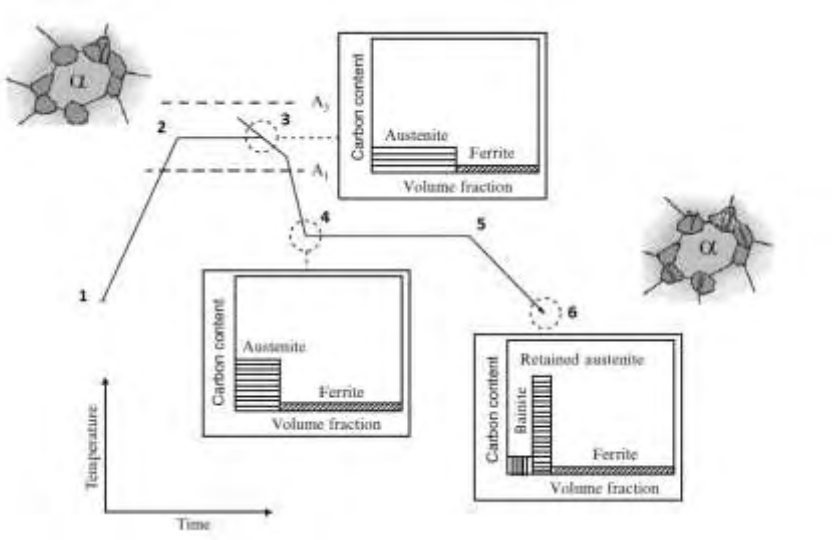

Figure 2.6: A schematic representation of the heat treatment performed for TRIP steels

- 1-2 HEATING: Recrystallization, carbide precipitation cementite dissolution
- 2-3 INTERCRITICAL ANNEALING: Creation of austenite ferritic structure
- 3-4 COOLING TO ISOTHERMAL BAINITIC TRANSFORMATION: Transformation to ferrite
- 4-5 BAINITIC HOLDING TIME: Transformation from austenite to bainite
- 5-6 COOLING TO AMBIENT TEMPERATURE.

2.5 Martensitic transformation

One of the most important features in TRIP steels is the transformation of the retained austenite to martensite. This transformation provokes a crystallographic change in the materials lattice by decreasing temperature, while strengthens the material structure. Martensite transformation prevails in steels where it can offer an outstanding combination of strength and toughness.

The martensitic transformation is a structural lattice transformation with three basic characteristics:

1. Diffusionless: Diffusion is not required for martensite transformation to take place, as a consequence the martensitic phase inherits the composition, the atomic order and the lattice defects of the parent phase (austenite) [9]. Martensite can form at very low temperatures, where

diffusion, even of interstitial atoms, is not conceivable over the time period of the experiment. Martensite plates can grow at speeds which approach that of sound in the metal. The totality of these observations demonstrates convincingly that martensitic transformations are diffusionless.

2. Displacive: The formation of martensite involves the coordinated movement of atoms. It follows that the austenite and martensite lattices will be intimately related. All martensitic transformations therefore lead to a reproducible orientation relationship between the parent and product lattices [10].
3. Martensite morphology is dominated by strain energy coming from lattice distortive shear: The shear dominated strain energy has a major effect on transformation kinetics and morphology of the transformation product. The martensite crystals are shaped in order to reduce strain energy.

According to the theory the change in crystal structure is followed by a homogeneous lattice deformation. The lattice from FCC (austenite formation) transforms to BCC but due to the carbon trapped in interstitial positions the lattice ends up in a BCT formation. The strain component which causes this distortion in the crystal structure is called the Bain strain. The shear at the interface occurs either by slip or twinning. Figure 2.7 presents a schematic representation of martensitic transformation.

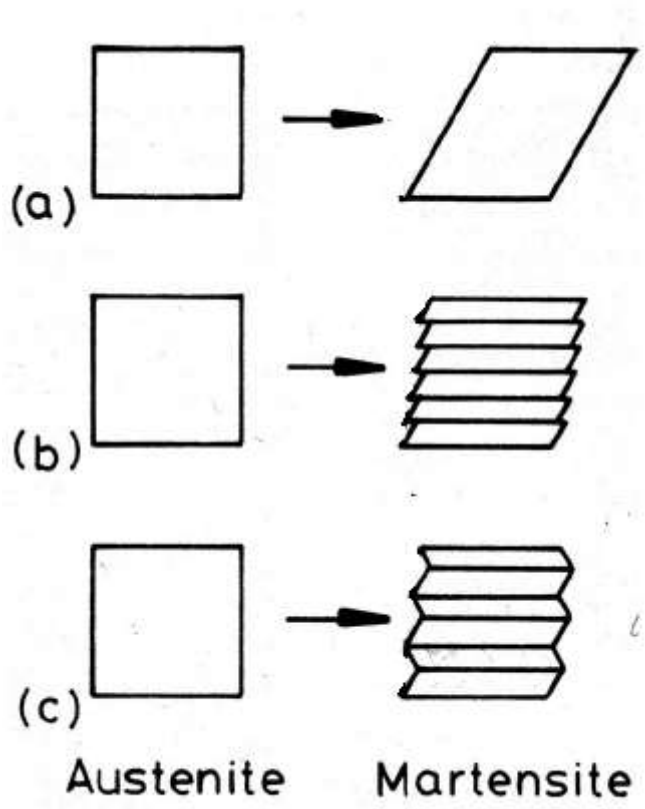

Figure 2.7: Schematic representation of martensitic transformation, a) the shape change predicted by Bain, b) shear at the interface between the austenite and the α' martensite, c) twining at the interface of austenite and α' martensite.

The Bain strain reveals the correspondence of lattice points between the parent crystal FCC and the martensitic crystal BCC. Figure 2.8 illustrates the correspondence cell (Bain model) embedded in two unit cells of the austenitic crystal FCC.

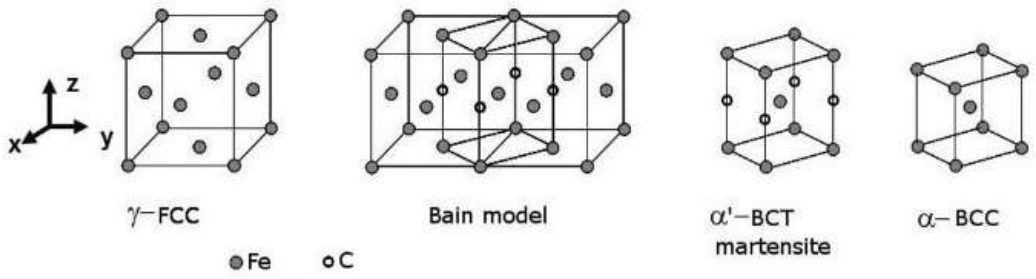

Figure 2.8: When the carbon atoms are inserted in the space between the atoms, and when considering two adjacent crystalline units, the Bain model will see a BCT-Martensite crystal frame if carbon atoms are present.

2.6 Transformation Plasticity

The fundamental mechanical properties of TRIP steels are supported by the ability to transform the remaining austenite with stress application. Martensitic transformation is triggered by external mechanical loading at high temperatures. The applied stress generates a mechanical driving force ΔG_{σ}, which aids the chemical driving force ΔG_{ch} and contributes to the critical driving force for martensitic nucleation [10]. As it can be denoted in the stress-temperature diagram of figure 2.9, there are two deformation modes occurring with the applied stress. For temperatures below the Ms the transformation of austenite to martensite happens spontaneously. Increasing the temperature, between the M_s and the M_s^{σ}, the transformation of the retained austenite occurs with the aid of stress applied which should not exceed the yield strength σ_y. The nucleation of the martensite is performing in the same nucleation sites were the spontaneous transformation, under cooling, would be created. This nucleation procedure is a stress assisted nucleation [11].

Above the M_s^{σ} temperature the material is plastically deformed, the stress values overcome the σ_y. According to other researchers, the transformation that occurs above the M_s^{σ} follows the yield strength σ_y. The stress at which transformation is initiated lies significantly below the relatively-steep stress-assisted transformation line extrapolated below M_s^{σ}. Therefore the nucleation occurring above M_s^{σ} is different in kind from the stress-assisted nucleation manifested below M_s^{σ}. This distinction defines that the that plastic deformation at σ_y and above introduces new, highly-potent sites which allow nucleation at appreciably lower stresses than in the case of stress-assisted nucleation. Hence, the nucleation above M_s^{σ} is considered to be strain-induced [11]. The M_d temperature defines the maximum temperature which martensite transformation cannot be induced by deformation; the driving force is so small that it is impossible to nucleate martensite. The M_s^{σ} temperature characterizes the stability of the austenite grains under mechanical force while the M_s characterizes the stability of austenite under cooling transformation. TRIP steels are stable at room temperature and without the mechanical contribution transformation starts at the M_s.

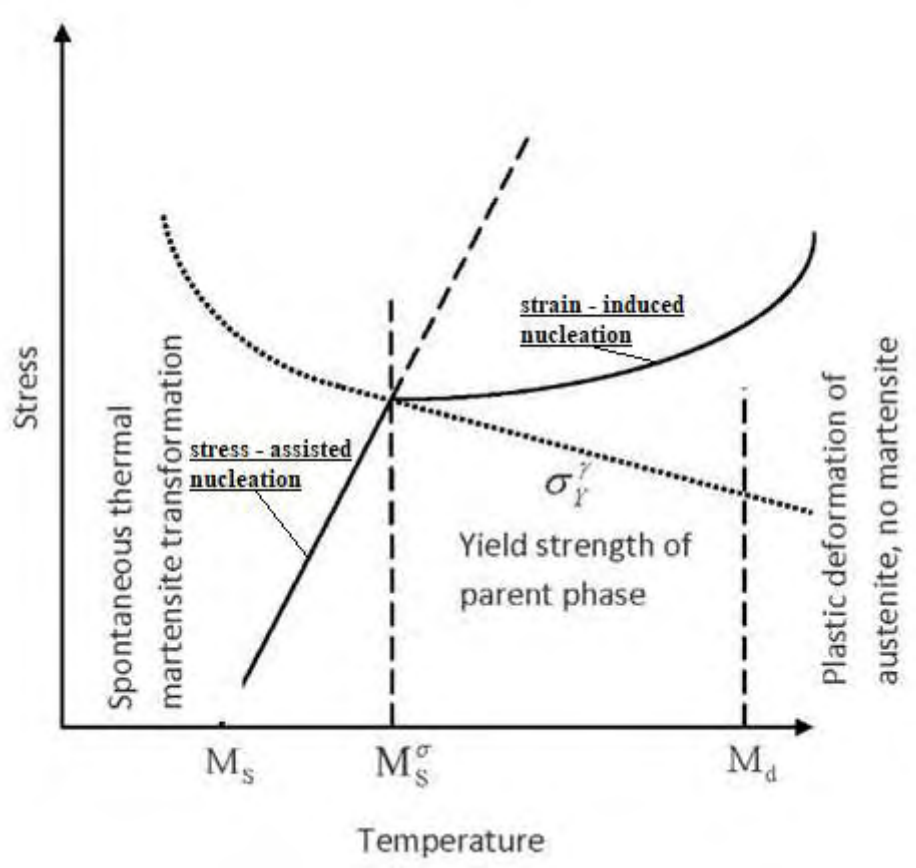

Figure 2.9: Schematic representation of martensitic transformation with the contribution of stress [12].

2.7 Stability of the retained austenite

The optimum TRIP effect is obtained by ensuring continuous transformation of RA to martensite throughout deformation, producing the best mechanical properties. Typical it can be deduced the higher amount of RA volume fraction the better mechanical properties. However, the mechanical properties of the steel also depend on the RA stability, which means the resistance to the mechanically induced martensitic transformation. There are several factors that affect the stability of the retained austenite. The most important is the concentration of stabilizing alloying elements in the austenite.

A common TRIP steel chemistry contains small additions of alloy elements which can help the austenite to be stabilized but also keep the austenite grain saturated with carbon. The hardenability of the ferrite can also be enhanced with the addition of alloying elements. The precipitations of the alloying elements prevent the formation

of carbides by enriching the austenite with carbon. The manganese is considered as austenite stabilizer, the austenite hardenability increases with the increase o Mn content. Also inhibits the formation of bainite and decreases the M_s temperature after the isothermal bainite transformation [13]. The silicon additions facilitate the enrichment of austenite with carbon increasing the stability and the volume concentration [14]. The aluminum affects similarly the diffusion of carbon as the silicon inhibits the formation of the bainitic transformation [15]. Research has shown that aluminum helps the carbon of the steel to remain inside the retained austenite leading to a bainitic-ferrite carbide free structure [6]. Those elements optimize the volume fraction of the retained austenite, increase the hardness of ferrite, control the precipitation of ferrite and slow the formation of pearlite before the bainite reaction. Higher stability of retained austenite allows the material to exhibit a progressive strain hardening in a stress strain curve allowing for increased elongation of the material [16].

The size of the retained austenite grains is another factor that controls the retained austenite stability. Smaller grains tend to be more resistant to transformation resulting to increased stability. The grain influences the interfacial energy for the formation of martensite and its decrease leads to a significant decrease in the M_s temperature. A retained austenite grain smaller than 0.01μm is useless for TRIP steels, since it will not transform to martensite, while that with a grain size larger than 1μm may be equally useless, since it will immediately transform to martensite upon cooling or during application of small stress [17], [18].

Different shapes of retained austenite also contribute in the stability factor. Structures having the same amount of retained austenite, but different shape morphologies exhibit different stability. It is observed that circular (equiaxed) microstructure exhibit faster transformation compared to the lath like (lamellar). Transformation of an elongated austenite grain would require the formation of many small martensite laths to compensate for the morphology of the grain because the laths are unable to cross grain boundaries. This transformation would result in a high interfacial area for the new martensite in comparison to the volume, thus increasing the interfacial energy component of the energy required for transformation. So elongated retained austenite present to have more stable grains. Also larger grains of retained austenite transforms faster to martensite [18], [19]. The shape morphologies

are influenced in the bainitic holding time. Circular structure has the ability to form high volume fraction but this value drops of quickly with shorter or longer holding times. Otherwise the elongated grains tend to hold their volume fraction in the bainitic holding time making them less sensitive [20].

Another factor that can increase the RA stability is strain rate deformation. Investigations carried out to clarify the effect of strain rate on the strain-induced transformation have indicated that the transformation is suppressed with increasing strain rate. This was explained in terms of adiabatic heating, which decreases the chemical driving force of the transformation according to studies [21].

2.8 Fracture of TRIP steels

As for other mechanical properties, the fracture behavior of TRIP steels has been found to be influenced by the TRIP effect as well as other microstructural parameters. From the available literature findings on tear resistance of TRIP steels it has been found in [22] that the transformation of retained austenite induces a plastic relaxation at the localized stress concentration of the crack tip which suppresses the void formation and stabilizes the crack extension. The fracture toughness behavior is influenced by the soft wide lath-martensite matrix containing small carbides and the effective plastic relaxation of the TRIP effect of the retained austenite suppressing void formation, crack growth and the cleavage fracture at the crack tip.

Further research on static fracture of TRIP steels has shown that the continuous phase transformation at the crack tip can be effectively simulated using modeling technics. This modelling technic investigates fracture behavior of TRIP 800 on a C(T) specimen under uniaxial loading [23].

In [24] a high alloy metastable TRIP steel with particle reinforcement of MgO and ZrO_2. was studied. The results showed that the toughness of the composite is primarily determined by the presence of reinforcement particles. The low interfacial strength between the steel and ceramic associated with small interparticle spaces leads to an accelerated fracture process and a low overall toughness.

2.9 Crack growth propagation in TRIP steels

Research on the fatigue crack growth behavior of TRIP steels has shown some interesting results about the propagation of the crack. A significantly higher resistance to fatigue crack growth attributed to the fraction of retained austenite. The measurement on the crack tip shows a decrease in RA fraction. The comparison of the experimental result was between an optimal and non-optimal heat treated TRIP steel [25].

Stress amplitude promotes austenite-martensite phase transformation during cycling loading. It is generally assumed that in TRIP steel strain-induced martensite formation in the crack tip plastic zone increases the amount of crack closure and that this is the reason for the lower fatigue crack growth rate. Plastic deformation of the crack flank can cause lower crack growth rates than expected. If crack closure occurs the deformation of the flanks makes them touch each other. This means that the stress does not represent the true stress on the crack tip [25].

It is also studied in [26] that the crack propagation path is depended on the microstructure. The crack tip might meet barriers on which it is deflected and then either runs along grain boundaries or right through the grains. These barriers arise from the composition in the presence of hard phases (bainite, austenite, martensite) dispersed in a ductile matrix (ferrite) and the strain-induced martensitic transformation. The effect of retained austenite transformation lowers the crack growth rate at the lower values of ΔK.

3 Experimental Program

3.1 Material

The TRIP 700 aluminum containing steel has been used for the investigation, which includes heat treatment, metallographic investigation and mechanical testing. The material was supplied in as-received condition with a chemical composition presented in Table 3.1, in sheet form with a thickness of 1.5 mm. The sheet was hot rolled and the initial percentage of the retained austenite in the microstructure was 15.8%.

Table 3.1: The chemical composition of the TRIP700 material.

C	Si	Mn	P	Al	S	Cr	Ni	Mo	Cu
0.202	0.348	1.99	0.009	1.07	0.0013	0.0038	0.017	0.011	0.044

3.2 Heat treatment

3.2.1 Preparation of heat treatment furnace

For the experimental procedure Thermawatt furnaces were used with non-exposed heating resistances and high density ceramic fiber insulation, having a maximum working temperature of 1000^{o}C. The furnaces were used for preheating the specimens and for the austenitization process. This procedure was performed in order to erase the previous microstructure by creating new materials with different RA characteristics via heat treatment. For the heat treatment process appropriate tanks were used that act as salt baths and are placed inside the heating furnace. The tanks were designed and manufactured in a workshop from 318 type stainless steel in order to minimize the oxidation effect due to exposure to high temperatures, with a thickness of 5mm. The tank geometry, which was assembled using TIG welding is shown in Figures 3.1, 3.2 and 3.3.

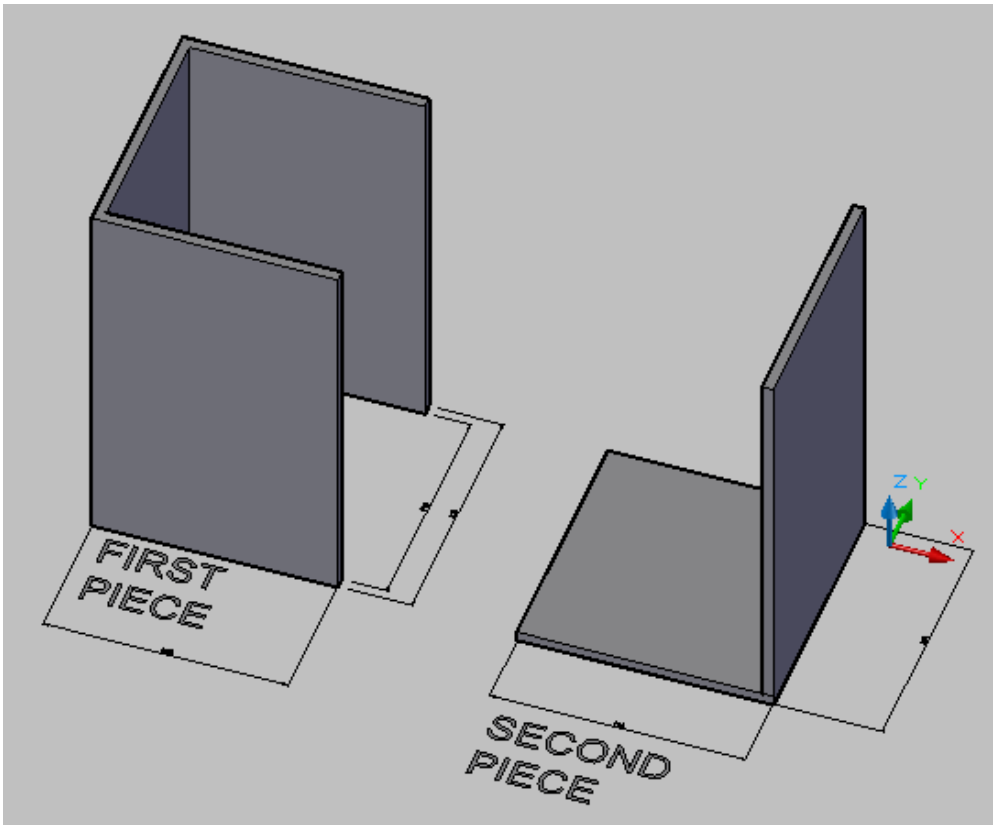

Figure 3.1: A schematic representation of the tank used in the furnace .

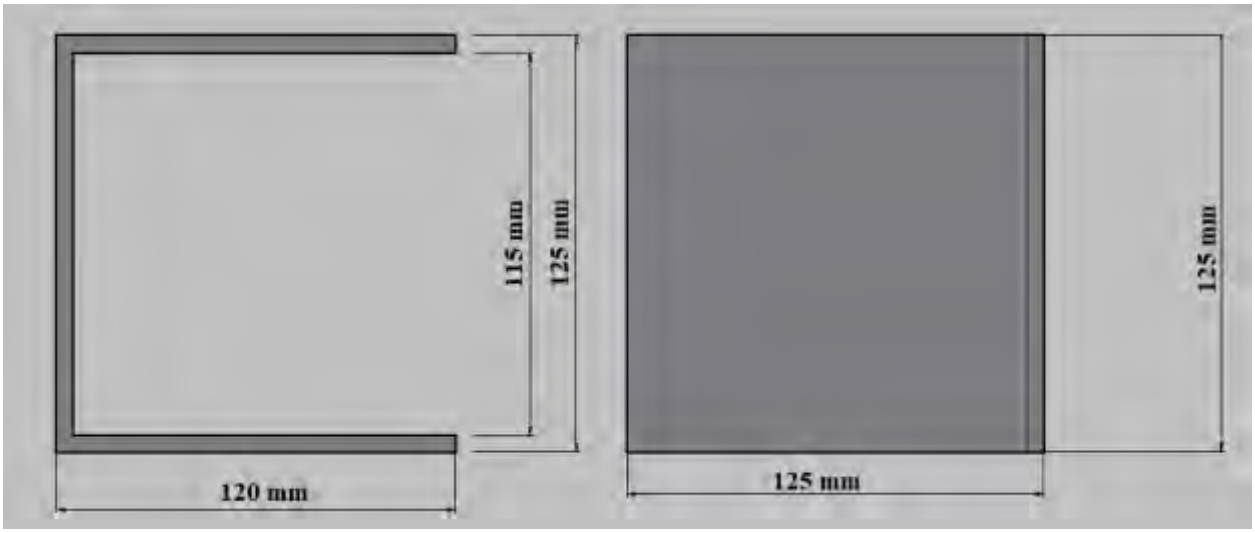

Figure 3.2: The tank geometry (dimensions, top view).

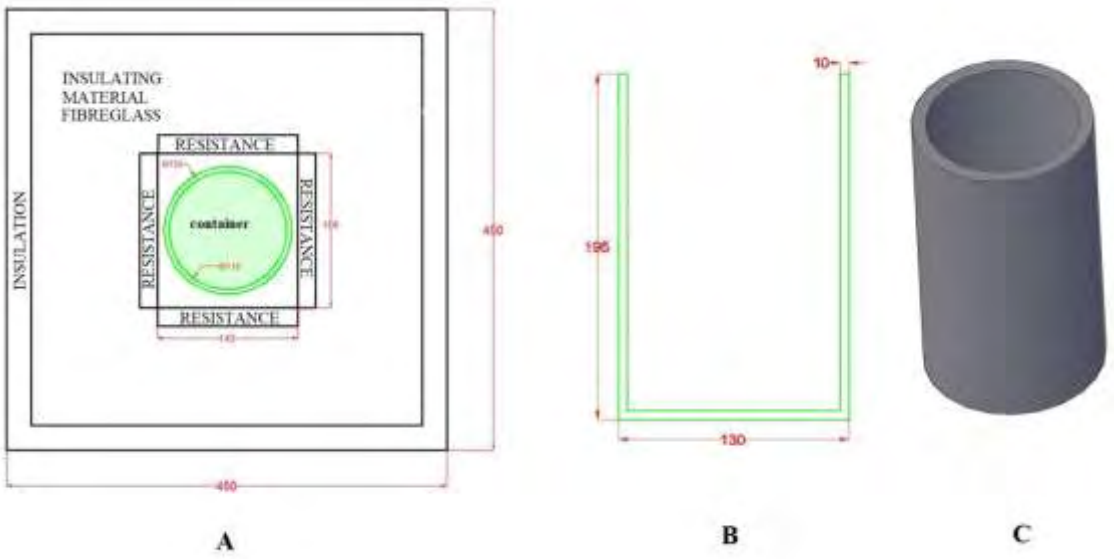

Figure 3.3: A) a schematic representation (top view) of the furnace with the tank situated in the middle, B) a section of the tank plane view (middle) and C) a 3D view of the tempering tank.

Prior to operation, the furnaces were serviced and had their damaged contents replaced. The electrical resistance was restored and placed inside the ceramic material with fiberglass around the chamber of the resistances. For more insulation a covering plate was placed on the top made from pressed fiberglass covered with fireproof cement for high temperature use as shown in figure 3.4. The control of the temperature inside the furnaces in order to achieve a uniform temperature distribution of the samples was accomplished by using two thermocouples.

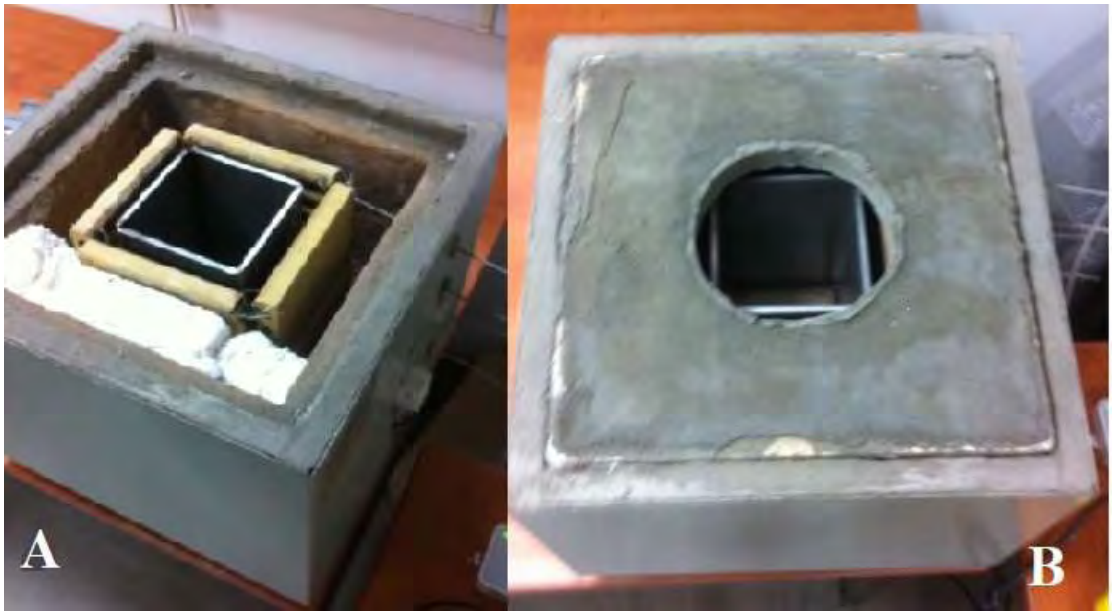

Figure 3.4: The furnaces, A) the ceramic chamber along with the container ready for fiberglass installation and B) ready for use

3.2.2 Salt baths

For the heat treatment process including the intercritical annealing and the isothermal bainitic transformation salt baths were used in order to achieve better temperature conduction, which according to the phase diagram (Figure 2.5.) provoke the microstructural changes. The salts were placed inside two metal tanks, one for annealing and the other for bainitic isothermal transformation. As the temperature increases the salts inside the tanks reach the melting point of 850^0C for the intercritical annealing and 160^0C for the BIT furnace.

The salt medium used for the intercritical annealing process was GS 750 [29], a product from Durferrit with working temperatures from 850^oC to 1000^oC. The main ingredient of the salt is Barium Chloride. In [27] it was found that decarburization of steel is prevented by adding a compound called R2 which contains Barium (when the specimens remain inside the salt baths for a long period) [28]. For the isothermal bainitic procedure AS 140 [27] salt was used, with working temperatures 160^oC to 540^oC. This salt is not recommended for use with workpieces which are heated up to above 950 °C and salts which contain more than 13 % KCN [29].

3.2.3 Design of heat treatments

The scope of the experimental procedure was to produce from the as received material with specific chemical composition, materials with variation in microstructure, specifically regarding the change in retained austenite volume fraction, morphology and stability.

The samples used for the first heat treatment procedures were cut in rectangle shapes with dimensions 2cm X 5cm. Their geometry included a small hole to facilitate for a quick transfer from one furnace to the other due to high temperatures, figure 3.5. The second heat treatment procedures included bigger rectangle shaped samples with dimensions 12cm X 10cm and 15.5cm X 10cm. In Figure 3.6, 3.7 the placement of the steel samples inside the chamber is shown prior to the heat treatment procedure. The uniform temperature distribution between the metallic plates inside the chamber was obtained by securing a uniform gap between each sample with the help of bolted connections at the corners. In total 21 samples were subjected to heat treatment process in order to prepare specimens for tensile and fracture testing

Figure 3.5: typical geometry of samples used in heat treatment

Figure 3.6: Arrangement of samples with bolted connections

Figure 3.7: Placement of steel samples inside the tank prior to the heat treatment process

The heat treatment which the TRIP samples have been subjected to include in total three steps, namely i) austenitization, ii) intercritical annealing and c) bainitic isothermal transformation are described in more detail below:

3.2.3.1 Austenitization

Austenitization process was performed in order to recrystallize the material and create a new microstructure. The temperatures and time for austenitization were selected from a number of trials and errors in order to avoid much of the oxidation effect of the material. The recrystallization was able to be achieved just above the Ac3 temperature. The samples were preheated in the front-load furnace, in 400^{o}C for 1 minute and then directly were deposited in the second furnace for the austenization process 950^{0}C for 4 minutes, then air cooling followed, figure 3.7.

Figure 3.7: Front load furnaces A) for preheating, B) for austenitization process

3.2.3.2 Intercritical Annealing

The selection of parameters for the intercritical annealing process was made according to G.N. Haidemenopoulos et al. [16]. The transformation temperatures of the material are Ac1:673^{o}C and Ac3: 913^{o}C. Following the austenitization process the samples were preheated again for 1 minute to 400^{o}C and subjected immediately to the furnace with salt bath at the temperature of 890^{o}C for 60 seconds

3.2.3.3 Bainitic Isothermal Transformation

After the completion of intercritical annealing the sample subjected again for the isothermal bainitic transformation at 400^{o}C A, and B, 120 and 820 seconds respectively, finishing with air cooling, figure 3.8. From each specimen a small sample was cut off and sent in Austria for RA measurements.

The second heat treatment procedure after the completion of the same intercritical annealing subjected in BIT, figure 3.9, table 3.2, with heat treatment “A” and “B” at 400^{o}C for 120 and 820 second respectively and then heat treatment “C” and “D” at 460^{o}C for 120 and 820 second respectively, finally air cooling followed. The specimens was sent to a workshop to be cut according to ASTM standards of the mechanical testing procedure which will be described in more detail below.

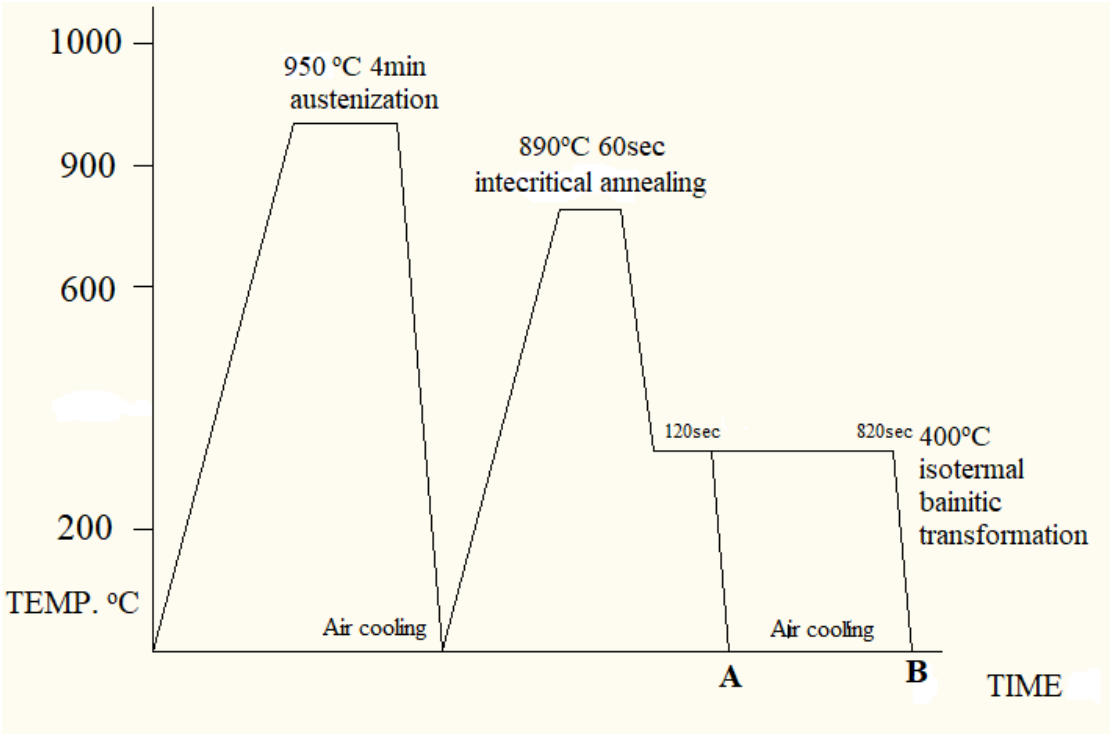

Figure 3.8: Time duration in the in the BIT treatment process

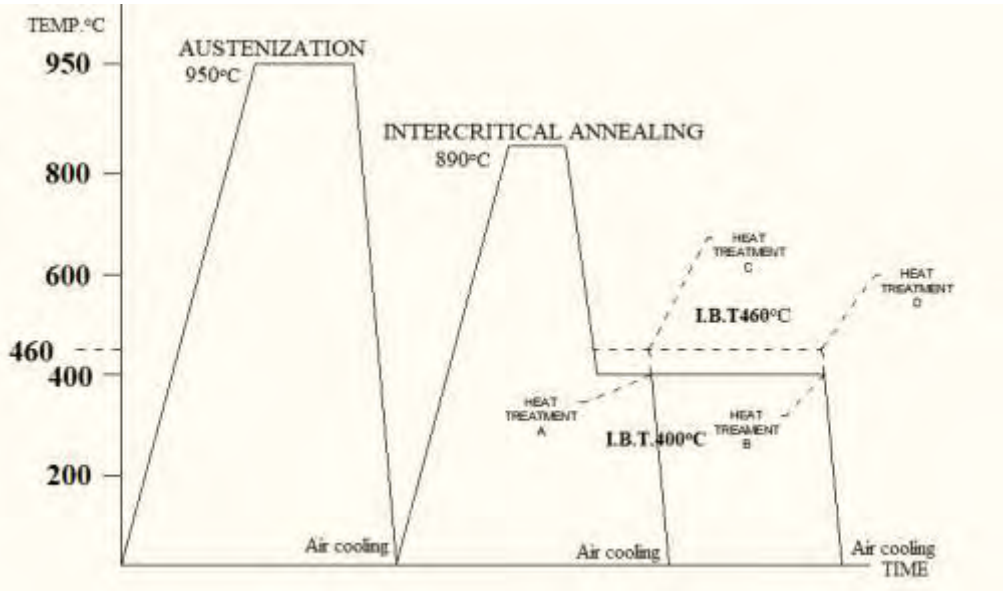

Figure 3.9: Temperatures used in the BIT heat treatment process

Table 3.2: Parameters used in the Heat treatments

Heat treatment	Austenization 950 °C	Intercritical annealing 890 °C	Isothermal Bainitic Transformation
A	4min	60sec	400 °C – 120sec
B	4min	60sec	400 °C – 820sec
C	4min	60sec	460 °C – 120sec
D	4min	60sec	460 °C – 820sec

3.2.3.4 Retained Austenite measurements

Following the heat treatment procedure RA measurements were performed to evaluate the initial volume fraction of the RA phase after the different heat treatment processes. The RA measurements were performed with the saturation magnetization method, in Voestalpine Steel Division GmbH, Linz, Austria, and. are presented in Table 3.3. The results indicate that the performed process leads to a reduction of the initial RA content compared to the as received TRIP 700 material which has 15.8% RA, but the differences obtained are not significant.

.

Table 3.3: Results of retained austenite volume fraction after heat treatments A and B.

Isothermal bainitic transformation time	A	B
	120s	820s
Retained austenite %	14.8%	12%

3.3 Metallographic inspection

For the metallographic investigation and in order to reveal the basic microstructural characteristics of the materials, an etching technique was used following grinding and polishing of small metallic samples of the heat treated steels. .

The samples were cut with Struers Labotom cutting equipment and the rough edges were trimmed with a medium grit paper. Then the samples were placed in a mould of resin to provide better handling for the grinding procedure and obtain a plane view in optical microscopy.

The purpose of the grinding technique is to gradually remove all the surface imperfections (for example rough edges, surface deformations) and reveal the real microstructure of the material. The procedure consists of grinding with silicon carbide paper starting from 120 and following 220, 500, 800 and 1000. Thus the surface roughness of the specimen diminishes gradually and the final goal is to create a plane microscopically surface. The next step included polishing of the surface with diamond

paste (1 μm) and lubricant on a fabric disk, creating a mirror like surface of the samples.

After grinding and polishing, the specimens were etched with 2% Nital (HNO3) for 3 seconds to reveal the grain boundaries. The Nital etching is used to visualize the grain boundaries (3ml HNO3 combined with 100ml of ethanol). The next etchant is 10% sodium bisulfide NA2S2O5 (10gr NA2S2O5 AND 100ml water), which is used to reveal separately the phases of martensite-austenite, carbon containing phases and ferrite by coloring them.

3.4 Mechanical testing

3.4.1 Tensile Tests

The mechanical properties of the materials were determined by uniaxial tensile tests according to ASTM E8 standard [30]. In Figure 3.10 the specimen geometry used for the tensile test is shown. The tests were conducted on the INSTRON 8801 (Figure 3.11), servo hydraulic testing system with a 100kN load cell. For the tensile tests an INSTRON axial extensometer was used.

Figure 3.10: Tensile test setup

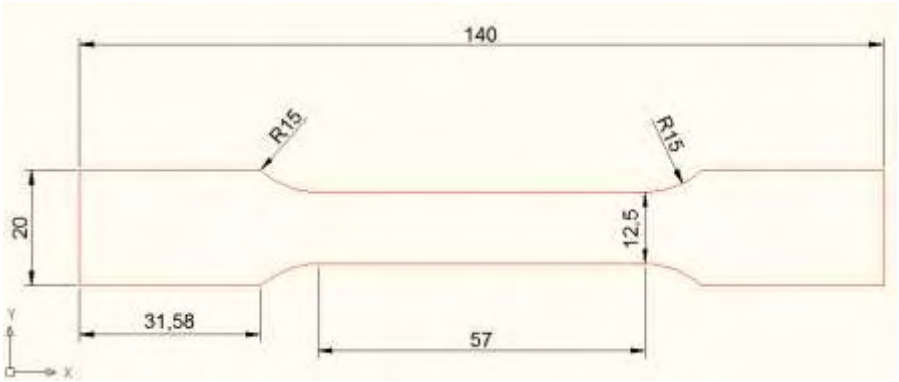

Figure 3.11: Tensile specimen geometry

3.4.2 Fracture resistance testing

Fracture resistance tests were conducted according to ASTM 561 [31] specification. The C(T) specimen geometry is given in Figure 3.12. Due to the small thickness of the material 1.5.mm an antibuckling device was used (Figure 3.13) in order to obtain valid K-results and to ensure no out of plane deformation takes place during K_I- mode testing. For this purpose two rigid metallic plates were attached on the specimen surface on both sides. Teflon was used between the surfaces of specimen and metallic plate to reduce the friction effect.

A COD extensometer was used to give a precise indication of the relative displacement between crack surfaces. The COD gauge was supported on the knife edge of the specimen, which was designed according to ASTM 399 [32] and was attached at the points V1, V2 presented in figure 3.14.

Prior to the fracture tests a precracking procedure was performed for the development of a physical crack of approximately 3mm length at the root of the notch. The tests were carried out with a displacement rate of 0.2mm/second.

For the evaluation of crack increment with increasing load, the elastic compliance method was used based on the guidelines of ASTM 561 specification [31].

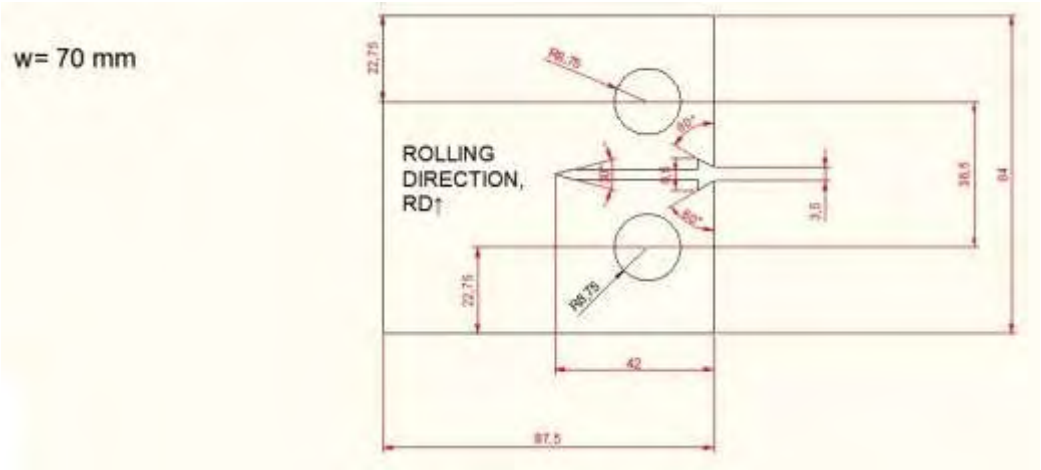

Figure 3.12: Compact Tension C(T) specimen geometry

Figure 3.13: Fracture resistance test setup

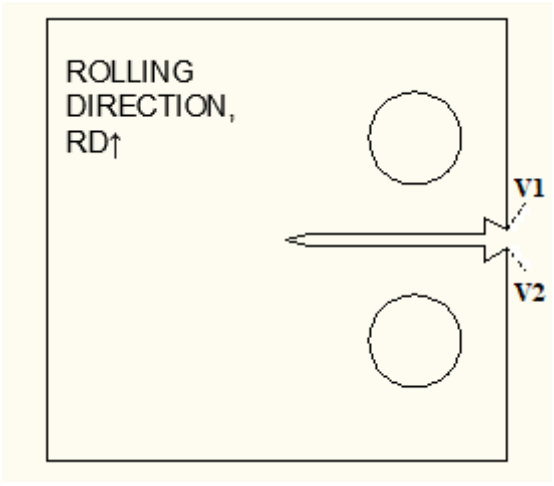

Figure 3.14: Points V1, V2 for the measurement of crack tip opening displacement.

3.4.3 Fatigue crack growth tests

The fatigue crack growth tests were carried under load control with a maximum and minimum stress of σ_{max}= 9 MPa and σ_{min}= 0.9 MPa. The specimen geometry used for the tests is presented in figure 3.12. The fatigue precracking for the development of a physical crack was 3.5mm. The same antibuckling configuration with the fracture tests for a valid K_I mode testing. The frequency used in the fatigue crack growth tests was 10 Hz and the stress ratio was R =0.1. COD measurements were performed at the outer specimen crack surfaces at points V1, V2 as shown in Figure 3.14.

The translation of the crack opening values to crack length was made with the elastic compliance method as described in the specification ASTM 647 [33]. The fatigue crack growth coefficients were obtained using the Paris equation 3.1 for a stress ratio R=0.1 in the form:

$$d\alpha/dN=C(\Delta K)^m \qquad (3.1)$$

The coefficients were evaluated with a stress intensity factor range between 16 and 25 MPa $m^{1/2}$ corresponding to Stage II fatigue crack growth.

4 Results

4.1 Microstructure

The microstructures of the materials in the as received condition and after the heat treatment process are presented in the micrographs of Figures 4.1-4.12. In the micrographs the material is etched by the solution, the tinting effect shows the retained austenite grains with white color, the ferrite grains with brown and blue color (the difference in coloring is because of the reflexion of the different crystallographic planes) and the small black regions correspond to the bainite phase.

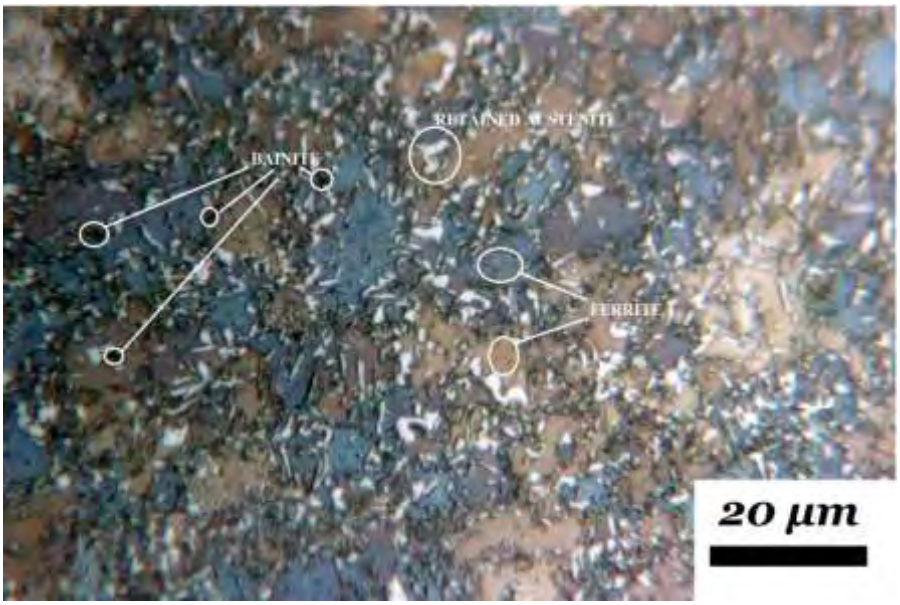

Figure 4.1: Specimen TRIP700 – As received

In Figure 5.1 the material microstructure in the as received condition is depicted. The retained austenite has a uniform dispersion and consists from bulky equiaxed grains. Its size is characterized from very small particles and larger particles. The average size has been measured in [34] as 0.7μm. The initial volume fraction of RA is 15.8%. The ferrite consists of larger grains with an average diameter of 9.47μm [34] and is the phase with the largest volume fraction, while the content of bainite in the as received state is low.

In figures 4.2, 4.3, the heat treatment A microstructure is presented. The retained austenite has almost uniform dispersion like the as received material. In microstructure A the number of large RA particles seems to be reduced compared to

the as received condition, however this has not been confirmed by grain size measurements in the present study. The bainite fraction seems not to be affected compared to the as received condition.

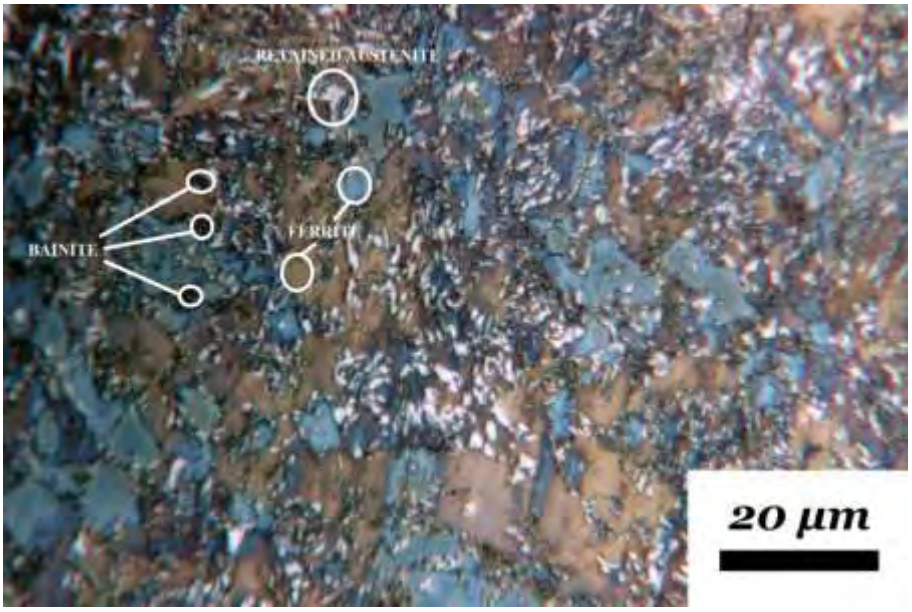

Figure 4.2: Metallography heat treatment A picture 1

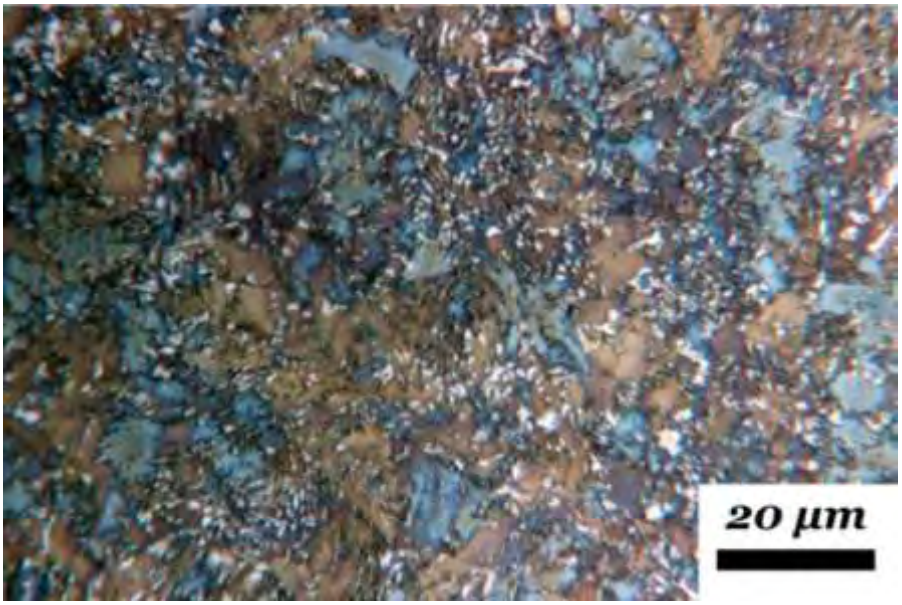

Figure 4.3: Metallography of heat treatment A picture 2

In figure 4.4 micrographs related to the microstructure after treatment B are displayed. The material in this case has a prolonged holding in the BIT region compared to the A treatment at the same temperature, leading to an increase of volume fraction of the bainitic phase. The retained austenite seems to consist of

smaller equiaxed grains, which should be expected to result in an increase of the stability of the RA.

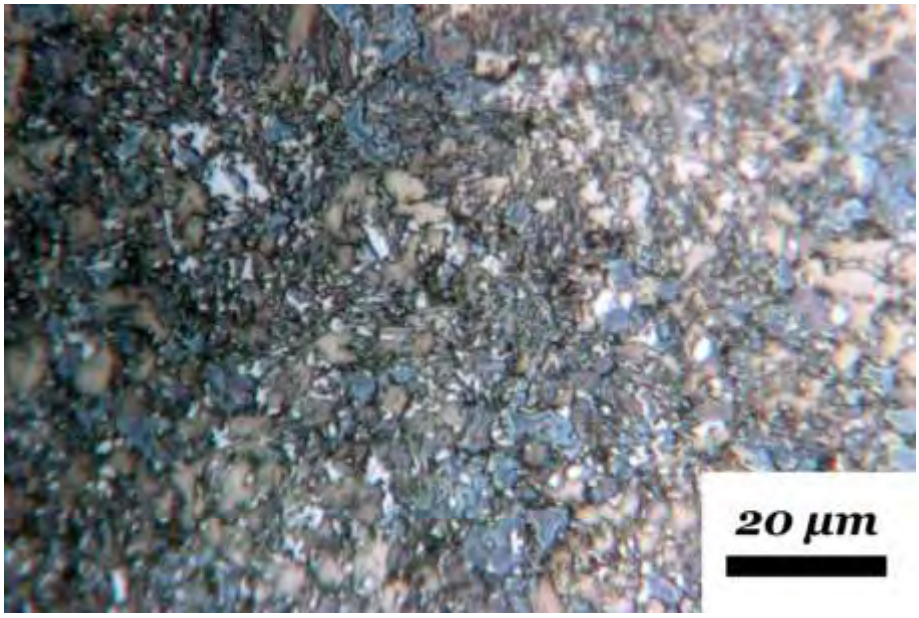

Figure 4.4: Metallography of heat treatment B

In figures 4.6, 4.7, the micrographs corresponding to the heat treatment process C are shown. The increase in the bainitic temperature causes more intense modifications in the microstructure morphology The retained austenite grain has a needle like formation and is characterized by a lamellar shape [19],[20]. The grains are almost equally dispersed. Moreover the bainite appears with coarser grains compared with the treatments A and B.

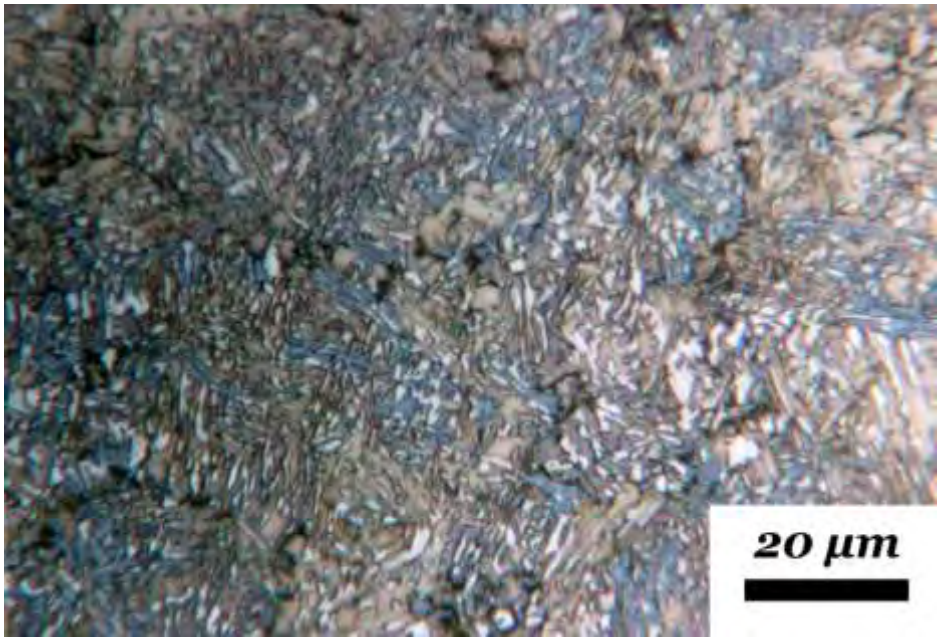

Figure 4.6: Metallography of heat treatment C picture 1

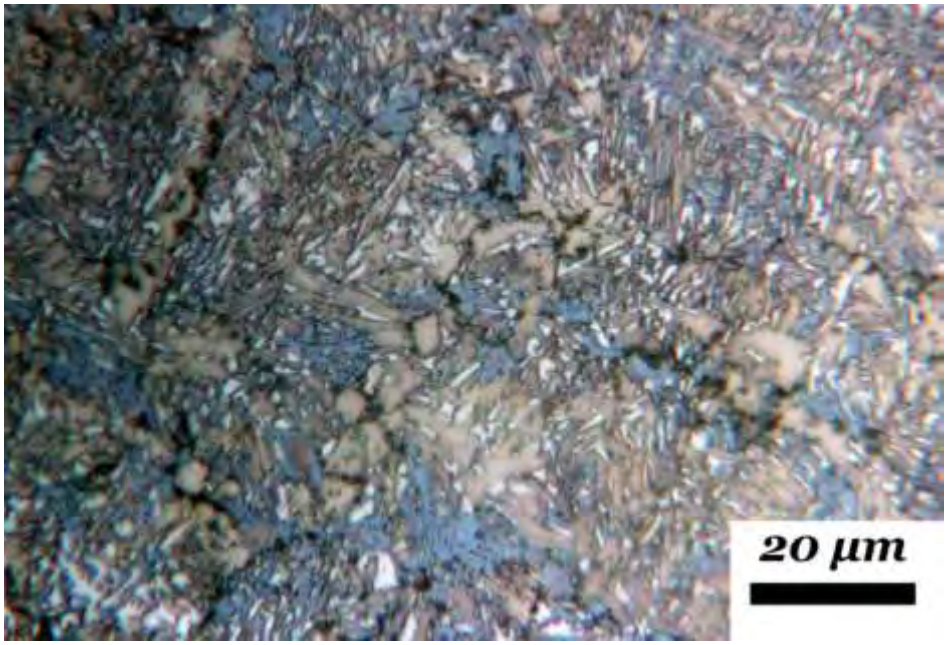

Figure 4.7: Metallography of heat treatment C picture 2

For longer duration in the BIT region, treatment D, the retained austenite grains decrease in size as shown in Figures 4.8 and 4.9 but the lamellar shape is kept although to a lesser extent. The dispersion of the retained austenite grains is uniform and the content of the bainitic phase appears to be higher than in the other microstructures.

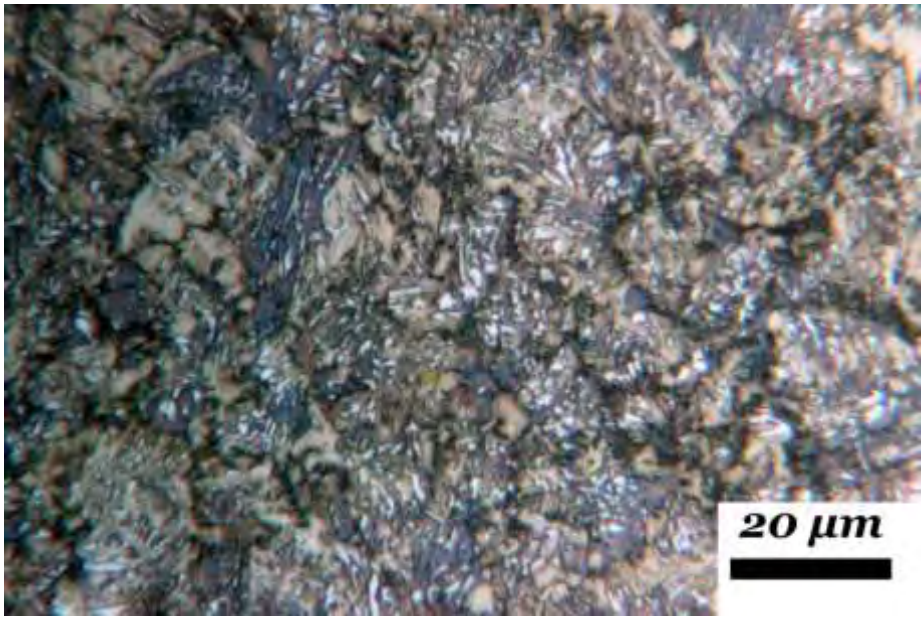

Figure 4.8: Metallography of heat treatment D picture 1

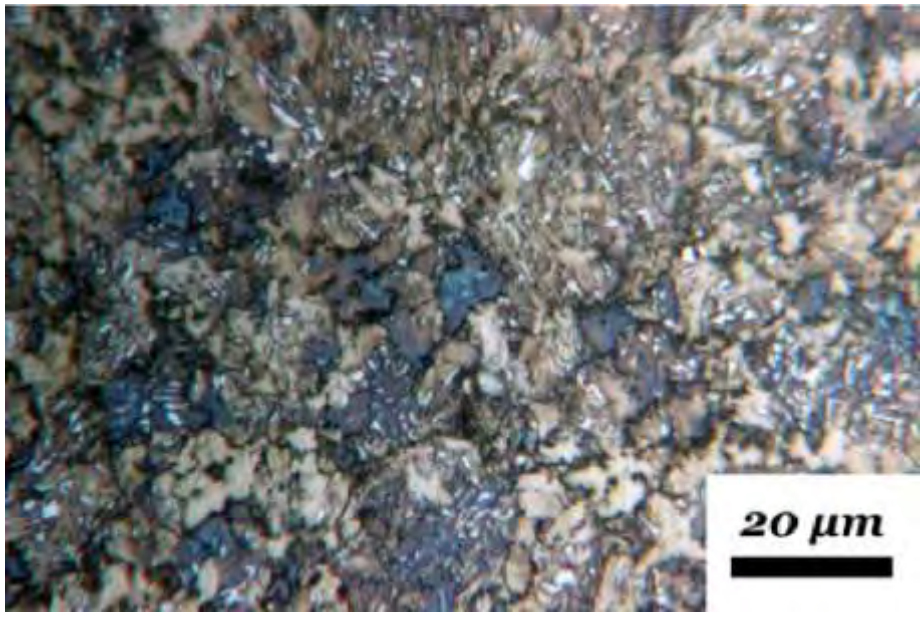

Figure 4.9: Metallography of heat treatment D picture 2

4.2 Tensile behavior

The engineering stress-strain curves resulting from the uniaxial tensile tests conducted on the heat treated materials are shown in figure 4.10 and values for individual mechanical properties are summarized in Table 4.1.

The material (AR) in the as received condition exhibits the highest uniform elongation (26.5%) compared to the heat treated materials, combined with a moderate strain

hardening exponent value (n=0.103). The uniform elongation value is reduced with a simultaneous increase in strain hardening after heat treatment processes C and D. The highest strain hardening value (n=0.18) and lowest uniform elongation is found in material C (16.7%). Heat treatment processes A and B contribute to the reduction of the strain hardening value compared to the as received material, but the uniform elongation is also slightly reduced. By comparing the strength characteristics, materials B and A have the highest yield strength values (550 and 534 MPa respectively), while the lowest yield strength belongs to material C with a value of 482 MPa.

From the obtained results it is obvious that the heat treatment process which influences the TRIP effect leads to different material behavior. For instance, the observed mechanical behavior suggests that the austenite transformation behavior is different in the examined materials. That is, in the case of AR material there seems to be a controlled transformation behavior (stable transformation rate with increasing strain) leading to a moderate strain hardening capacity and high uniform elongation prior to necking.

In materials C and D transformation of austenite to the hardened martensitic phase is expected to occur at early deformation stages, resulting in higher strain hardening and reduced elongation. Although the lamellar type RA structure increases generally the stability of RA [19,20], the increase in size of RA particles and content obtained by observing the microstructures in Figures 4.6 – 4.9 may act contrariwise, thus assisting the transformation phenomenon [13]. In A and B steels, the stability of austenite against transformation is higher compared to the as received material and the associated strain hardening low. This is confirmed by measurements of the M_s^{σ} temperatures performed in [35], where the material B examined here, showed the highest RA stability followed by material A and the material in as received condition. The uniform elongation does not seem to benefit compared to the as received condition.

.

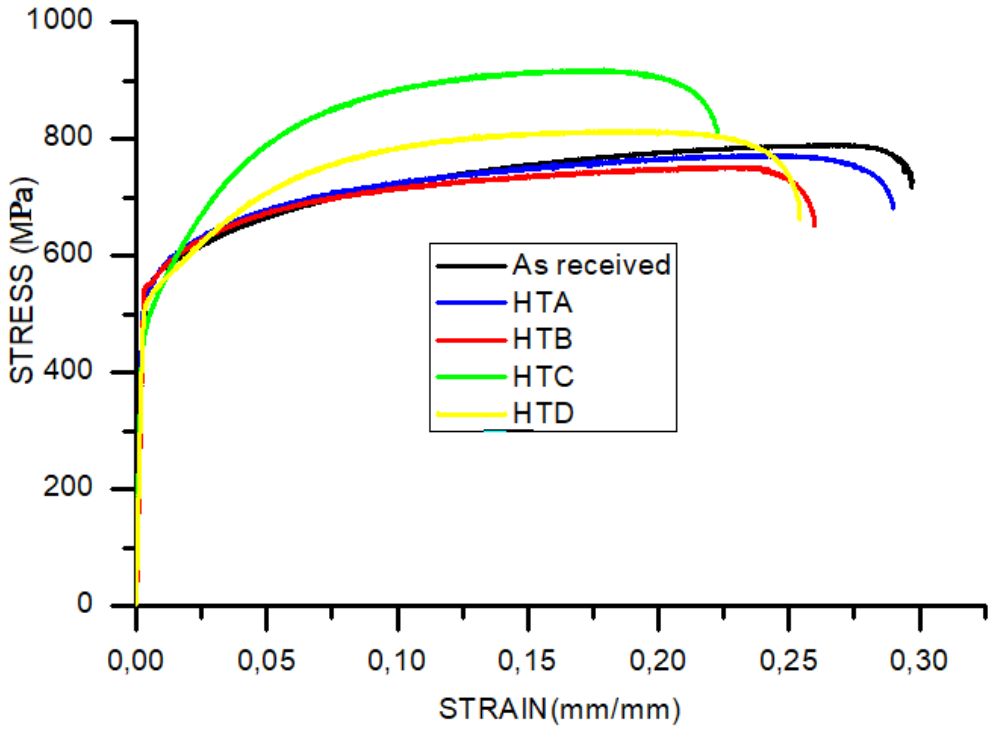

Figure 4.10: Engineering stress-strain curves for all the different microstructures

Table 4.1: Tensile properties for all the microstructures

MATERIAL	Yield strength σ_y (MPa)	Ultimate tensile strength σ_{UTS} (MPa)	Strain hardening exponent (n)	Uniform elongation U_a (mm/mm)	Total elongation U_{50} (mm/mm)
As received	523	789	0,103	0,265	0,297
H.T. A	534	770	0,092	0,22	0,29
H.T. B	550	751	0,08	0,214	0,259
H.T. C	482	917	0,18	0,167	0,22
H.T.D	526	812	0,13	0,198	0,254

4.3 Fracture resistance tests

The crack growth resistance curves plotted as force vs crack opening displacement curves for the investigated materials are shown in Figure 4.11. For the specimen geometry used the maximum crack length for a valid stress intensity factor range according to LEFM conditions was calculated as a_o=28.45 mm , which corresponds to

an increment of 4 mm from the machined notch tip. Measurements of the K resistance value have been made until the valid data according to the ASTM 561 compliance, figure 4.11.

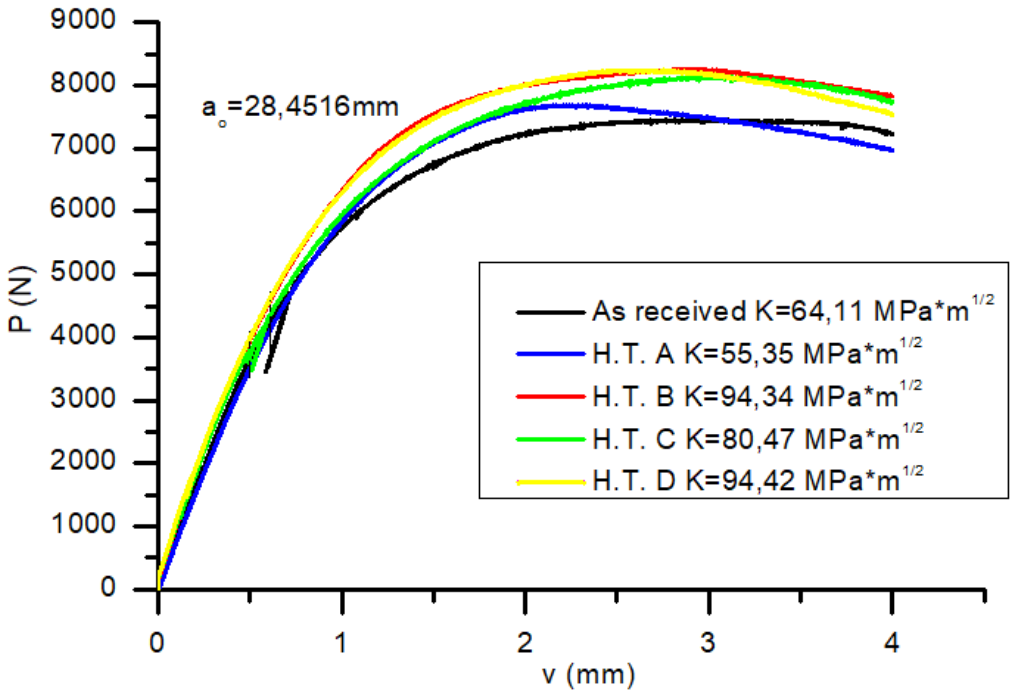

Figure 4.11: Comparative Load vs crack tip opening displacement diagram for the different materials

By observing the fracture behavior of the C(T) specimens for each material in Figure 4.11, differences in fracture behavior may be noticed. The material in as-received condition exhibits the lowest resistance for opening of the crack surfaces compared to the other materials, while B and D materials show the highest fracture resistance potential. The maximum force achieved for the specimen configuration of Figure 4.12 belongs to material B and was determined as P_{max}=8250kN, while the lowest was for the as received material P_{max}=7430kN.

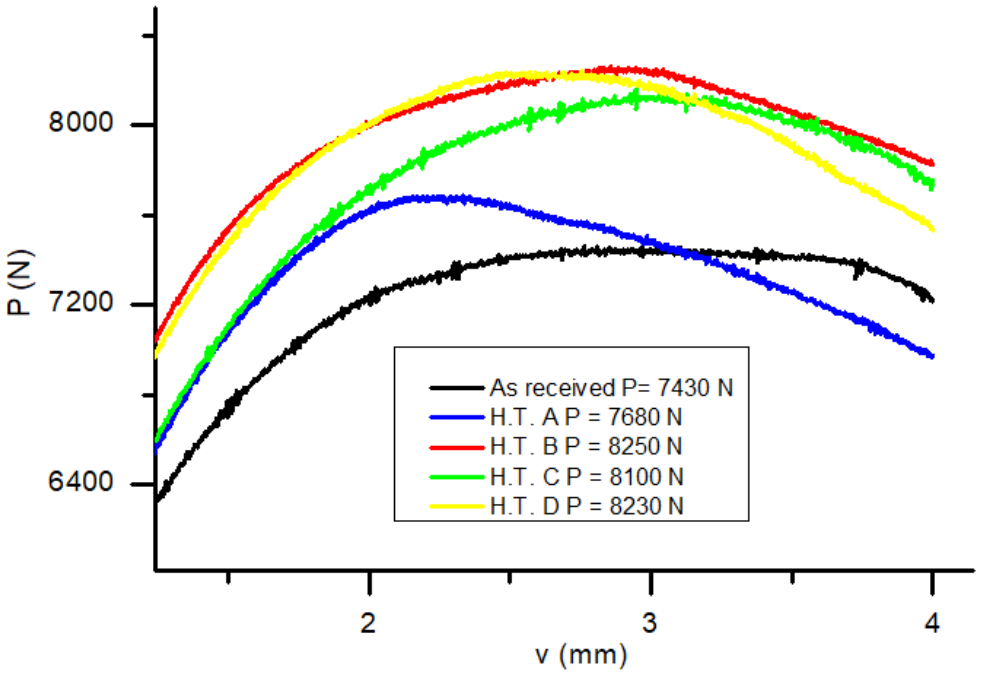

Figure 4.12: Magnification of Load vs COD diagram at the region of maximum load

The observed behavior of TRIP steels may be explained by taking into account the transformation effect occurring at the plastic zone ahead of the crack tip. Taking into account that the specimen geometry is the same for each material, the plastic zone is influenced by the material's yield strength value. The low yield strength value of material C is expected to contribute to higher plasticity ahead of the crack tip compared to the other materials, which may influence the transformation process and produce martensite which is a harder phase. On the other hand the lath type microstructure of the austenitic phase in material C (Figures 4.6, 4.7) suggests that the austenite grains are more stable against transformation compared to the other microstructures. The increased stability of austenite with a lath type microstructure has been reported in several investigations [19, 20]

In TRIP steels the fracture resistance has been generally inversely associated with the transformation effect and RA content since fracture has been associated with void coalescence and growth along martensite and ferrite phases [36]. Also resistance to crack growth has been linked with increased RA stability [36]. Therefore material C exhibits an intermediate fracture resistance compared to the other materials. The as received material does not present a very stable RA microstructure, as suggested by the larger RA particles and critical transformation temperature [35] and also has a

relatively high initial RA amount. These parameters contribute to the low fracture resistance behavior. The latter is high in materials B and D, where a relatively stable RA phase is accompanied by smaller initial RA content and smaller transformation process zone.

The combination of a stable RA particle may assist the fracture resistance of material D.

4.4 Fatigue crack growth rates

The fatigue crack growth increment of the materials is plotted against the number of cycles in figure 4.13.The crack growth curves show that specimens from the heat treated materials C and D exhibit higher fatigue life of crack propagation until failure, while A and B materials show inferior crack growth performance. The as received material exhibits an intermediate fatigue crack growth behavior.

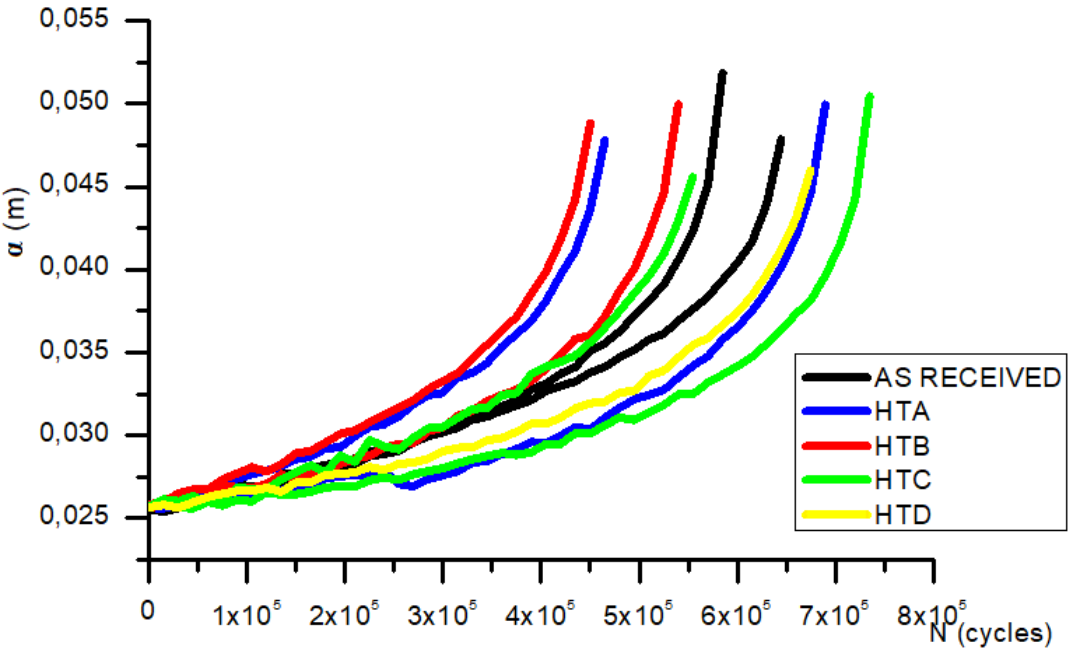

Figure 4.13: Fatigue crack growth α (m) vs N number of cycles

The dα-dN vs ΔK graphs for the different materials are presented comparatively in Figure 4.14 and the associated Paris coefficients are given in Table 4.2. The fatigue crack growth rates present minor differences at high ΔK values, but differences at early stage II fatigue crack growth are more evident. The C and D materials show a more damage tolerant behavior under cyclic loading for ΔK values up to 20 MPam ^{½}

compared to the other steels, while the as received material exhibits slightly lower crack growth rates compared to the heat treated steels A and B. Although the TRIP effect has been associated with a retardation of fatigue crack growth in TRIP steels [25, 26, 37], the effect has been found to be more effective at high ΔK ranges where there is significant plasticity to facilitate the transformation process [38]. On the other hand, highly laminated structures in TRIP steels (showing similarities to the C and D case examined here) have been found to decelerate the rate of the growing crack due to phenomena related with crack closure (e.g increases surface roughness at the crack path) [39]

At high ΔK values (above 20 MPam $^{1/2}$) the differences in fatigue crack growth rates of the materials diminish. Taking the above under consideration the obtained behavior may be due to the insufficient transformation taking place at stress intensity factor range values below 20 MPam $^{1/2}$ and from the microstructural effects arising from the morphology of retained austenite phase (lamellar type) which contribute to increased fatigue crack growth resistance.

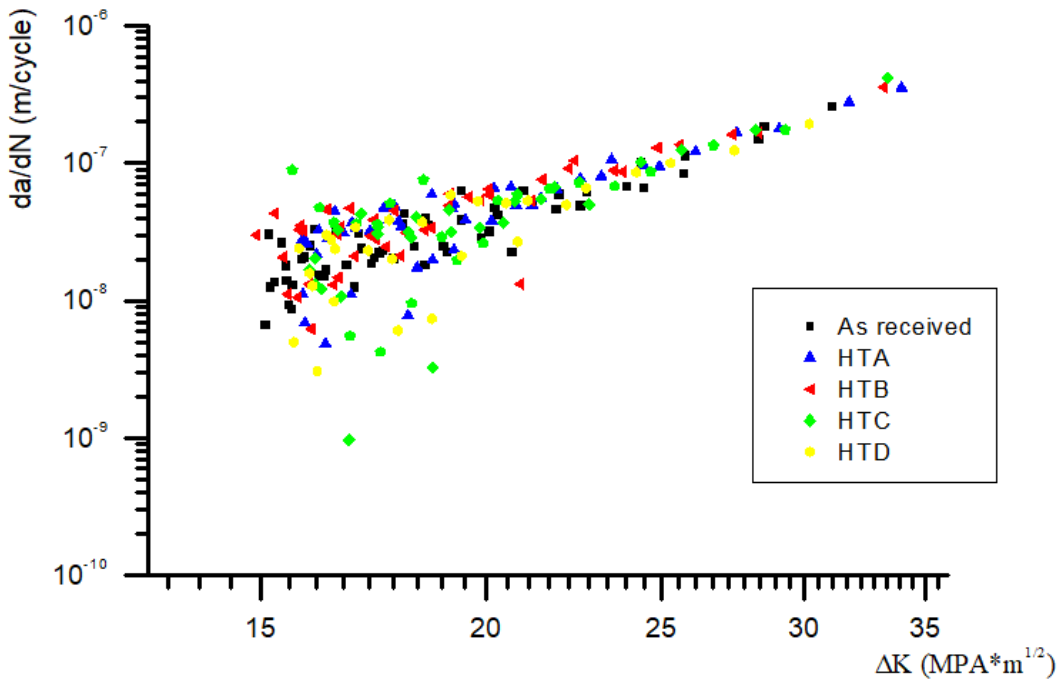

Figure 4.14: Fatigue crack growth rates vs Stress intensity factor range

In stage II the crack growth is propagating according to the Paris equation, $\frac{da}{dN} = C(\Delta K)^m$, where the coeficients of each specimen are presented in table 4.2.

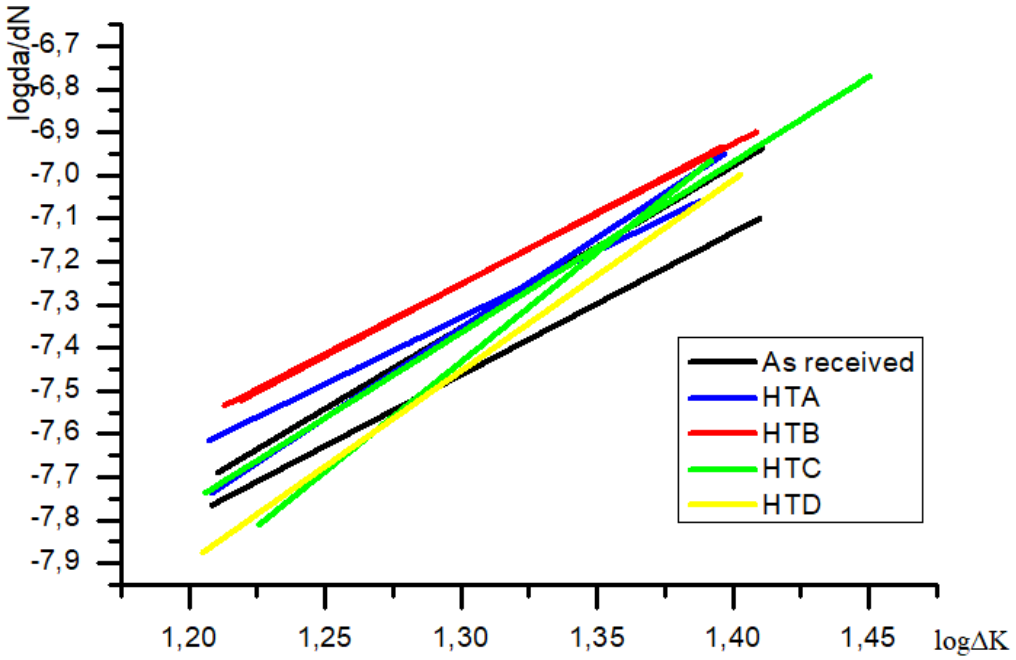

Figure 4.15: Linear fitting approximations in Stage II fatigue crack growth

Table 4.2: Paris coefficients as obtained from the from da/dN - ΔK diagram

MATERIAL	m	C (mm/cycle* MPa $m^{1/2}$)
As received	3.53	$9.73*10^{-13}$
HTA	3.62	$2.47*10^{-12}$
HTB	3.28	$3.04*10^{-12}$
HTC	4.52	$1.63*10^{-13}$
HTD	4.43	6.3*10-14

5 Conclusions

The influence of heat treatment parameters in the Bainitic Isothermal Transformation on the microstructural characteristics and fracture mechanical behavior of TRIP 700 steel have been experimentally evaluated. The main findings of the experimental study may be summarized in the following:

- The microstructural investigation revealed that increasing time in the BIT region results in a reduced content of retained austenite with a finer grain structure but negligible differences in grain morphology. On the other hand the content of the bainitic phase increases with increasing process time.
- The increase in temperature in the BIT region is associated with the change in grain morphology of the retained austenite. The bulky equiaxed grains are replaced by a lamellar type microstructure and further increase of the bainitic phase content.
- The tensile behavior is directly related to the obtained RA microstructure following the heat treatment procedure. Material C with a lamellar austenite exhibits higher strain hardening compared to the other materials probably due transformation occurring due to the larger RA particles, which reduce the stability and higher RA content. Materials A and B exhibit a more stable behavior against transformation resulting in low strain hardening, while the as received material has the highest uniform elongation as a result of a RA microstructure with moderate stability enabling a progressive transformation with increasing tensile strain.
- The fracture behavior of materials seems to be negatively affected by the RA transformation, which in this case is localized at the crack tip and not bulk transformation as in the case of the tensile test. The as received TRIP 700 steel shows an inferior fracture resistance compared to the other materials. Materials B and D with a smaller RA particle tend to show limited transformation potential in the confined plasticity region at the crack tip, exhibiting an overall better fracture resistance.
- The damage tolerance behavior under cyclic loads does not benefit significantly from the transformation effect at low stress intensity factor

ranges. Other microstructural influences as the lamellar grain morphology of austenite seem to assist the fatigue crack growth behavior at low ΔK values

REFERENCES

[1] World Auto Steel. *Advanced High Strength Steel (AHSS) Application Guidelines*, Technical Report, Volume 4.1, (2009)

[2] THE STEEL WIRE, POSCO, URL: http://globalblog.posco.com/tag/giga-steel/

[3] S. Keeler, K. Menachem, *Advanced high strength steels applications guidelines*, World Auto Steel Volume 5.0, (2014)

[4] S.I. Kim, Y.H. Jin, J.N. Kwak, K.G. Chin, *Influence of cooling process after hot rolling on mechanical properties of cold rolled TRIP steel.* Material Science & Technology, Pittsburg (2008), p 1784-1802

[5] I. Samajdar, E. Girault, B. Verlinden, E. Aernoudt, V. Humbeeck, *Transformation during intercritical annealing of a TRIP assisted steel*, ISIJ International, Volume 38 (1998), No. 9, p, 998-1 006

[6] N. Fonstein, *Advanced high strength sheet steels*, Springer International Publishing, Switzerland, (2015)

[7] S. Nemecek, Z. Novy, H. Stankova, *optimization of heat treatment of TRIP steels*, La Metallurgia Italiana, (2006), p 47-51

[8] G. D. Chrisoulakis, D.I. Pantelis, *Science and technology of metallic materials*, Papasotiriou, (2003)

[9] G. N. Haidemenopoulos, *Physical Metallurgy*, Tziola, (2007)

[10] H. K. D. H. Bhadeshia, *Worked Examples in the Geometry of Crystals*, The Institute of Metals, 2nd edition, (2001), p51-69

[11] G. B. Olson, M. Cohen, *A mechanism for the strain induced nucleation of martensitic transformations*, Journal of the Less-Common Metals, *(1972)*, p107-118

[12] URL: http://what-when-how.com/dynamic-behavior-of-materials/dynamic-thermo-mechanical-response-of-austenite-containing-steels-dynamic-behavior-of-materials

[13] I. I. Bellas,*Study of strain-induced transformation in low-alloy TRIP steels*, MSc Thesis, In Department Of Mechanical Engineering, University of Thessaly, (2017)

[14] P.J. Jacques, E. Girault, Ph. Harlet, F. Dellannay, *the developments of cold-rolled TRIP-assisted Multiphase steels. Low Silicon TRIP-assisted Multiphase steels,* ISIJ International, Volume 41, No. 9, (2001), p 1061–1067

[15] P.J. Jacques, E. Girault, A. Mertens, B. Verlinden, J. van Humbeck, F. Delannay, *The developments of cold-rolled TRIP assisted steels. Al alloyed TRIP assisted multiphase steels,* ISIJ International, Volume 41, No. 9, (2001), p 1068–1074

[16] G.N.Haidemenopoulos, A.T. Kermanidis, C. Malliaros, H.H. Dickert, P. Kucharzyk, W. Bleck, *On the effect of austenite stability on high fatigue of TRIP 700 steel,* Materials Science & Engineering Volume A 573 (2013) p 7-11

[17] J. Wang, S. Van Der Zwaag, *Stabilization mechanisms of retained austenite in transformation induced plasticity steel,* Metallurgical And Materials Transaction A, Volume 32A, (2001), p 1527-1539

[18] S. Chatterjee, Transformations in TRIP-assisted Steels: *Microstructure and Properties, Darwin College*, Ph. D. Thesis, University of Cambridge, (2006)

[19] J. Chiang, J.D. Boyd, A.K. Pilkey, *Effect of microstructure on retained austenite stability and tensile behavior in aluminum-alloyed TRIP steel,* Materials Science & Engineering, Volume A 638 (2015) p.132–142

[20] J. B. R. Lawrence, *The effect of phase morphology and volume fraction of the retained austenite on the formability of transformation induced plasticity steels,*MSc Thesis, Queen's University Kingston, Canada (2010)

[21] Z.He,Y.He, Y.Ling, Q. Wu, Y.Gao, L.Li, *Effect of strain rate on deformation behavior of TRIP steels,* Journal of Materials Processing Technology, Volume 212 (2012) p 2141–2147

[22] J. Kobayashi, D.Ina, A.Futamura, K.-i. Sugimoto, *Fracture toughness of an advanced ultrahigh-strength TRIP-aided steel,* ISIJ International, Volume 54, No. 4, (2014) p 955–962

[23] A.Soulami, K.S. Choi, W.N. Liu, X. Sun, M.A. Khaleel, Y. Ren, Y. D. Wang, *Predicting fracture toughness of TRIP 800 using phse properties characterized by in-situ high energy x-Ray diffraction,* Metallurgical And Materials Transactions A, Volume 41A, (2010), p 1261-1268

[24] R. Eckner, M. Krampf, C. Segel, L. Krüger, *Strenght and fracture behavior of a particle reinforced transformation toughened TRIP steel/ZrO_2 composite,*

Russian translation published in Mekhanika Kompozitnykh Materialov, Volume 51, No. 6 (2016), p. 1007-1026

[25] X.Cheng, R. Petrov, L. Zhao, M. Janssen, *Fatigue crack growth in TRIP steel under positive R-ratios,* Engineering Fracture Mechanics, Volume 75, (2008), p 739–749

[26] W. Mosselman, *The influence of the martensite content on the fatigue crack growth rate in TRIP and Dual phase steels*, MSc Thesis, Department of Material Science Engineering, Delft University Of Technology, (2007)

[27] Durferrit salts and auxiliary products, URL: *http://www.nitriersalze.com/en/salt-bath-heat-treatment.html* Product catalogue

[28] V. Cain, *High temperature creep behavior of Niobioum bearing ferritic stainless steels,* MSc Thesis, Department of Mechanical Engineering, Cape Peninsula University of Technology, (2005)

[29] URL: http://www.nabertherm.com/produkte/details/gr/thermprozesstechnik_2-warmbadoefen

[30] ASTM E8, *Standard test method for tension testing of metallic material*, (2002)

[31] ASTM E 561, *Standard practice for R-curve determination,(1998)*

[32] ASTM E399, *Standard Test Method for Linear-Elastic Plane-Strain Fracture Toughness K_{Ic} of Metallic Materials,* (2012)

[33] ASTM E647, *Standard test method for measurement of fatigue crack growth rates,* (2000)

[34] P.I. Christodoulou, A.T. Kermanidis, D. Krizan, *Fatigue behavior and retained austenite transformation of Al-containing TRIP steels,* Journal Of Fatigue, (2016), p 220-231

[35] I. TSATALIOS, *Design of experimental procedure and evaluation of M_s^{σ} in Aluminum containing TRIP steel*, Diploma Thesis, In Department Of Mechanical Engineering, University Of Thessaly, (2017)

[36] G. Lacroix, T. Pardoen, P.J. Jacques, *The fracture toughness of TRIP-assisted multiphase steels,* Acta Materialia Volume 56, (2008), p 3900–3913

[37] G. R. Chanani, S.D.Antolovich, W. W. Gerberich, *Fatigue crack propagation*

in TRIP steels, Metallurgical Transactions, Volume 3, (1972), p 2661-2672

[38] A. Trudel, M. Levesque, M. Brochu, *Microstructural effects on the fatigue crack growth resistance of stainless steel CA6NM weld*, Engineering Fracture Mechanics, Volume 115, (2014), p 60–72

[39] Z.Zhang, M. Koyama, M.M. Wang, K. Tsuzaki, C. C. Tasan, H. Noguchi, *Effects of lamella size and connectivity on fatigue crack resistance of TRIP-maraging steel*, International Journal of Fatigue, Volume 100, Part 1, (2017), p 176-186